Physics – Uspekhi **42** (9) 847 – 869 (1999)

REVIEWS OF TOPICAL PROBLEMS PACS numbers: 13.25.Ft, **13.85.–t**, 14.20.Rq, 14.40.Lb

Physics of charmed hadrons

S V Semenov

Contents

Abstract. The twenty five years that have passed since the experimental discovery of the first charmed particle have been extremely successful for the physics of charmed particles. In the 30 odd experiments conducted over this period, a large number of states of charmed mesons and baryons have been observed, over a thousand decay channels studied, and lifetimes measured. In the present paper, basic experimental results are reviewed and prospects for the near future are discussed.

1. Introduction

In 1964, the idea of extending the SU(3) symmetry, which included three flavors of quarks (u, d, and s), to SU(4) symmetry and introducing a quark of a fourth flavor, the c quark, was proposed [1]. Such an idea made it possible, in particular, to achieve symmetry between the leptons and quarks known at the time. In the same year, SU(4) multiplets of mesons and baryons were classified [2]. The proposal to carry out a search for charmed (supercharged) particles based on the multileptonic events in neutrino experiments was also presented at roughly the same time [3]. Six years later Glashow, Iliopoulous, and Maiani [4] explained the following effects by introducing the c quark: strong suppression in the nature of flavor changing neutral currents and the small difference in the masses of the K_S and K_L mesons [1].

In 1974, a new meson with a mass of about 3.1 GeV/c^2 was discovered simultaneously in the experiments at two particle accelerators in the US (the Brookhaven proton synchrotron and the Stanford electron – positron collider). Each group of researchers gave their own name to the new meson. The Brookhaven group headed by Samuel C C Ting called it the J particle [6], while the Stanford group headed by B Richter called it the ψ particle [7]. Hence the double name J/ψ. It is known without any doubt that the J/ψ is a vector meson that is the ground state of a pair consisting of a c quark and a $\bar{c}$ quark. Since the J/ψ contains c and $\bar{c}$ quarks simultaneously, it became known as a meson with hidden charm. At almost the same time the Stanford group discovered the 2S state of the $c\bar{c}$ pair, or the $\psi(2S)$ with a mass of about 3.7 GeV/c^2 [8]. The next year a group of experimenters using the DORIS accelerator in Germany discovered, in the DASP experiment, the 1P levels of the $c\bar{c}$ state [9]. Finally, in 1976, the MARK I experiment at the SPEAR accelerator (USA) revealed the existence of particles with open charm, i.e., containing only a c quark ($\bar{c}$ quark) together with a light antiquark (quark): the D^0 and D^+ mesons [10, 11]. A detailed description of this initial period of discoveries and studies of charmed particles can be found in the collection of articles *Adventures in Experimental Physics*, volume 5 [12]. There the participants

S V Semenov State Scientific Center of Russian Federation
'Institute for Theoretical and Experimental Physics',
ul. B. Cheremushkinskaya 25, 117259 Moscow, Russian Federation
Tel. (7-095) 129 96 06
E-mail: ssemenov@iris1.itep.ru

Received 18 January 1999
Uspekhi Fizicheskikh Nauk **169** (9) 937 – 960 (1999)
Translated by E Yankovsky; edited by L V Semenova

[1] A review of papers on charmed quarks published prior to the discovery of the J/ψ meson can be found in book [5] by L B Okun.

recall the various events in the fascinating story of these discoveries.

The study of charmed mesons (and later, charmed baryons) became an extremely fruitful area of particle physics. The properties of charmed particles have been studied successfully using electron – positron colliders and in the interactions of high-energy beams of photons, neutrinos, and hadrons with fixed targets.

The present review deals with the data concerning only open charm. Section 2 is a brief summary of the main experimental detectors used in studies of charmed particles. Section 3 is devoted to the main quark diagrams of the decay of charmed mesons and baryons. The experimental results of charmed hadron spectroscopy are presented in Section 4, while the data on lifetimes of charmed hadrons are discussed in Section 5, where there is also a qualitative explanation of the relationships, obtained in experiments, that link the different lifetimes of hadrons. Sections 6 and 7 are devoted to the results of studies of leptonic and semileptonic decays of charmed particles, and Section 8 discusses the most interesting results obtained by studying the numerous nonleptonic decays of charmed hadrons. The experimental results of the search for $D^0\bar{D}^0$ mixing and CP symmetry violation in D-meson decays are reviewed in Section 9, where the results of the search for rare decays are also discussed. Finally, Section 10 is a brief review of new experimental projects in the studies of properties of charmed particles.

The review does not cover the problem of fragmentation of charmed particles (detailed information on this topic can be found in Ref. [13]). Neither does it discuss the progress in studies of the properties of mesons with hidden charm, J/ψ, ψ' etc., conducted over the last decade at the SPEAR collider. This accelerator operated with electron – positron collision energies equal to the mass of the J/ψ or one of the excited states of the ψ meson. These studies constitute a separate broad area of the physics of charmed particles (see Ref. [14]).

2. Experimental detectors for studying the properties of charmed particles

Before we discuss the experimental results in detail, let us briefly explore the main types of experimental detectors used in studies of charmed particles. Most charmed particles were discovered in experiments involving electron – positron colliders. The experiments also yielded abundant information about the numerous decay channels of such particles.

At the end of the 1970s and the beginning of the 1980s the MARK III collaboration produced many results in the studies of properties of D mesons. The experiments were carried out using the SPEAR accelerator with a total energy of colliding electrons and positrons equal to the mass of the $\psi(3770)$ meson. This meson decays, with an almost 100% probability, to $D^0\bar{D}^0$ and D^+D^- pairs. In order to study the properties of the D_s mesons, which have a large mass, the energy of the colliding beams was increased to 4.14 GeV, which is somewhat higher than the $D_s\bar{D}_s$-pair production threshold. This provided favorable background conditions for the experiments because in view of an energy deficit the $D\bar{D}$ pairs were produced without accompanying hadrons. At present the BES experiment [16], which is part of the BEPC accelerator in Beijing, operates under the same conditions. The BES collaboration studies in detail the properties of D_s mesons at a total energy of the colliding beams somewhat higher than 4 GeV.

The experiments done in the 1980s at the PETRA (Germany) and PEP (USA) colliders at a total electron–positron energy of 15 – 20 GeV and at DORIS (Germany) and CESR (USA) rings at energies of each beam of about 5 GeV continued the detailed study of the decay rates of charmed mesons and hadrons, measured the lifetimes of mesons, and detected many new states of charmed hadrons. The production cross section of charmed particles in the $e^-e^+ \to c\bar{c}$ process is inversely proportional to the square of the energy of the colliding particles measured in the center-of-mass system (with the exception of the region of resonant production of a Z boson with a mass of about 91 GeV/c^2, in whose decay charmed particles are produced with a high probability). As a result, at the operational energies of the DORIS and CESR accelerators, the charmed-particle production cross section is approximately ten times larger than at the energies of the PETRA and PEP accelerators. The ARGUS experiment [17] at the DORIS collider and the CLEO experiment [18] at CESR contribute the most to the study of properties of charmed particles with the use of electron – positron colliders.

Finally, a large number of charmed particles have been detected using the electron – positron collider LEP at CERN (Switzerland) in the ALEPH [20], DELPHI [21], L3 [22], and OPAL [23] experiments. The total energy of the beams of the LEP accelerator was equal to the mass of the Z boson. The quantitative data on charmed mesons detected in different electron – positron collider experiments are listed in Table 1. Note that the number of charmed baryons produced in the ARGUS, CLEO, and LEP experiments is approximately ten times smaller than the number of charmed mesons.

Using the ARGUS detector [17] as an example (Fig. 1), we can acquaint ourselves with the main parts of practically all detectors used in electron – positron collider rings. The ARGUS detector is a universal magnetic 4π spectrometer designed for solving a broad spectrum of physical problems. In addition to studying charmed particles, the ARGUS group obtained very interesting results concerning the physics of B mesons and τ leptons [24] and new data on the spectroscopy of mesons with hidden charm, and studied various aspects of charmed particle fragmentation. The ARGUS detector was used for detailed studies of spectroscopy of light mesons in reactions caused by the interaction of two virtual photons [24]:

$$e^+e^- \to e^+e^-\gamma^*\gamma^* \to e^+e^-X\,.$$

Table 1. Number of charmed mesons produced in the most successful experiments involving electron–positron storage rings.

Experiment	Energy in the center-of-mass system, GeV	Number of charmed mesons produced
MARK III [15]	3.77; 4.14	$\sim 5\times10^4$ $D^0\bar{D}^0, D^+D^-, D_s\bar{D}_s$
BES [16]	4.03	6×10^3 $D_s\bar{D}_s$
ARGUS [17]	~ 10.6	5×10^5 $D^\pm, D^0(\bar{D}^0), D_s^\pm$
CLEO [18]	~ 10.6	10^7 $D^\pm, D^0(\bar{D}^0), D_s^\pm$
ALEPH [20], DELPHI [21], L3 [22], OPAL [23]	~ 91	$\sim 2\times10^5$ $D^\pm, D^0(\bar{D}^0), D_s^\pm$

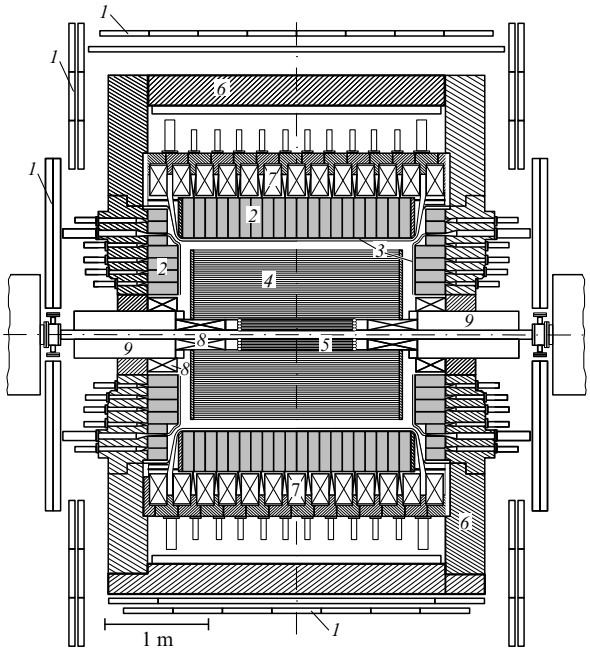

Figure 1. ARGUS detector: *1*, muon chambers; *2*, shower counters; *3*, time-of-flight counters; *4*, drift chamber; *5*, vertex chamber; *6*, magnet yoke; *7*, solenoid coil; *8*, compensation coils; and *9*, mini-beta-quadrupoles.

The detector was used to register hadrons, leptons, and photons and to determine, with good accuracy, the particle momenta. Two drift chambers yielded information about the tracks of charged particles. A more precise vertex chamber filled with gas under high pressure made it possible to attain a spatial resolution higher than 25 μm in measuring the coordinates of a charged-particle track. In the main track detector, a large cylindrical drift chamber 1.7 m in diameter, the tracks of charged particles were reconstructed in space with an accuracy of about 200 μm. The error in measuring the momenta of the charged particles did not exceed 1%. The measurement of the ionization losses of the particle energy in the drift chamber provided information about the type of particle (e, μ, π, K, and p). Additional information about the type of particle could be obtained by analyzing the data supplied by the time-of-flight system surrounding the drift chamber. The time of flight was measured with an accuracy of 220 ps. By combining these two sources of information the separation of particles by type could be substantially improved; most important, charged kaons could be reliably distinguished from charged pions up to 0.7–0.8 GeV/c in momentum.

To separate the electrons and photons and to measure their energy, the time-of-flight system was surrounded by an electromagnetic calorimeter, which consisted of alternating plates of the scintillator 5-mm thick and Pb plates 1-mm thick. Traveling through the dense lead layers, a primary particle (i.e. a particle entering the calorimeter) participates in electromagnetic interactions, as a result of which many secondary electrons are produced. These electrons then enter the scintillator layers. The energy of the primary particle is determined from the energy lost by the secondary electrons in the scintillator layers. The particle energy was determined with a 10% accuracy.

The magnetic field of the detector was generated by a current flowing through normal (i.e. nonsuperconducting) coils and amounted to 0.8 T. By increasing the strength of the magnetic field one could ensure a higher accuracy in determining the particle momenta. However, particles with relatively small momenta would follow a helical trajectory in a magnetic field and finding their momenta would be impossible. Since D mesons in electron–positron colliders are produced with a momentum of order 1–2 GeV/c, among their decay products are often particles with small momenta (100–200 MeV/c). The loss of such particles substantially reduces the probability of complete reconstruction of a D meson from the decay products.

Muon proportional chambers, used to detect muons, which are particles with minimum ionization losses of energy in matter, were placed on the outer side of the magnet.

To this day the CLEO detector [18], an integral part of the electron–positron storage ring CESR with a 10.6-GeV center-of-mass energy of the colliding particles, continues to operate effectively. Over a period of about 20 years, the CLEO detector underwent several modifications, which increased its capacity to identify particles and made it possible to operate in the conditions of a significant increase of the luminosity of the electron–positron storage ring CESR. At present most results have been obtained via the CLEO II modification [19]. CLEO II (Fig. 2) is a magnetic spectrometer with a perfect system of particle identification and a system of measuring the energy of electromagnetic particles. The detector incorporates a track system for detecting charged particles. The system is surrounded by

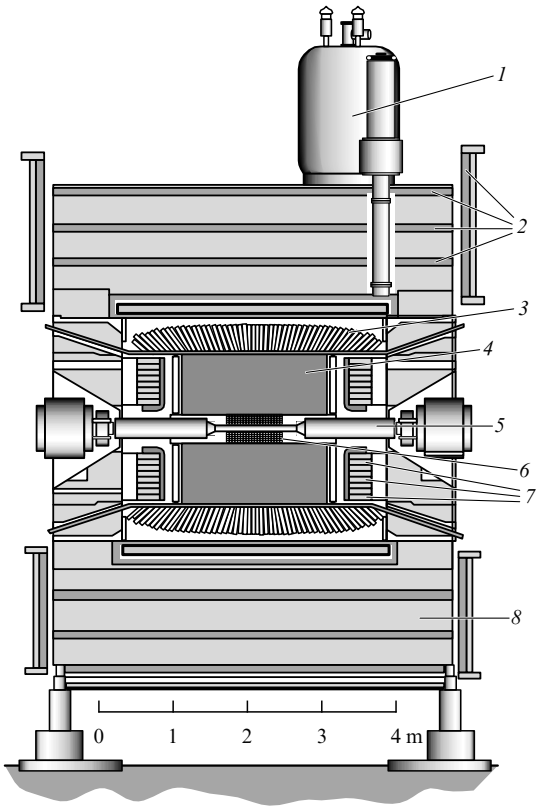

Figure 2. CLEO II detector: *1*, helium reservoir; *2*, muon chambers; *3*, shower counters; *4*, drift chamber; *5*, mini-beta-quadrupoles; *6*, vertex chamber; *7*, time-of-flight counters; and *8*, magnet yoke.

scintillator counters for measuring the time of flight of particles, and an electromagnetic calorimeter consisting of 7800 crystals of cesium iodide doped with thallium and used to measure the energy of photons and electrons. The track system makes it possible to measure particle momenta with an accuracy of 0.6%. The accuracy of measuring of the photon energy by the electromagnetic calorimeter varies from 4.2% at an energy of 100 MeV to 1.4% at 5 GeV. The electromagnetic calorimeter allows distinguishing, against background, neutral particles (π^0, η, and η') according to the photon decay channels. Using the information about energy losses to ionization in the drift chamber and time-of-flight data, the experimenters are able to separate pions from kaons up to 1.1 GeV/c at the 2σ level. These parts of the detector are placed inside a superconducting solenoidal magnet generating a 1.5-T magnetic field. The wire chambers for detecting muons are built into the magnet's yoke itself.

The described experiments allowed researchers to achieve results in studying charmed particles primarily due to the universal nature of the detectors. They not only made it possible to distinguish between particles of different types but also to measure the particle energy with high accuracy. Perfect identification of particles and, in particular, the capacity of the detectors to separate kaons from pions, have played a key role in selecting D mesons, which mainly decay to final states containing K mesons. The good energy resolution made it possible to reconstruct the D mesons from the decay channel being studied at a smaller contribution of the background from random combinations of particles that imitate a D meson (what is known as a combinatorial background). The experimental detectors covered almost the entire solid angle of 4π, when resulted in a significant increase in the number of D mesons and hence made it possible to study rarer decays. The more favorable background conditions in electron – positron colliders also contributed to new results. In electron – positron interactions, charmed particles are produced in approximately one inelastic interaction out of three. This, obviously, facilitates the discrimination of the signal above the combinatorial background and has huge advantages over fixed-target experiments, where charmed particles are produced in only one interaction out of several hundred.

However, the experimental detectors attached to electron–positron colliders have limited capacity for measuring the lifetimes of charmed particles. Such particles are produced in colliders with relatively small momenta ($\sim 1-2$ GeV/c) and travel only short distances before decaying. Since the lifetime of a particle is determined by the distance between the vertex of the primary interaction and production of the charmed particle to the decay vertex of that particle, a large relative error in measuring the distance leads to a large relative error in determining the lifetime.

The most precise measurements of lifetimes of charmed particles were conducted in experiments in which the beam of energetic particles (photons and hadrons) interacted with the nuclei of a fixed target. In such experiments, the charmed particles produced as a result of the interaction acquired large momenta due to the boost of the energy in the direction of the motion of the beam particles and, hence, had time to cover several times larger distances from production to decay than in experiments involving colliders. Nevertheless, even in such experiments the distance from the point of production to the point of decay for charmed particles amounts to several millimeters, and measuring distances with high accuracy requires using ultra-accurate vertex detectors that make it possible to determine the coordinates of the decay point to within several tens of micrometers. The advantage of using fixed target also becomes evident in studies of processes in which the time dependence of the decay of particles is investigated (e.g. in studying $D^0\bar{D}^0$ mixing). Modern experiments operating with fixed targets contribute significantly to research in the field of the decay of charmed particles, although such experiments are hindered by complex background conditions. For instance, when a pion or proton interacts with the target nuclei, charmed particles are produced in one interaction out of a thousand. When a photon interacts with the target nuclei, the production of charmed particles is several times more frequent, but still only in one interaction out of two hundred. Table 2 lists the data on the number of charmed particles reconstructed in experiments with fixed target.

Table 2. Number of charmed particles reconstructed in experiments with fixed target.

Experiment	Beam particles	Average energy of particles incident on target, GeV	Number of reconstructed charmed hadrons
E691 [25]	γ	90 – 260	$\sim 10^4$ $D^{\pm}$, $D^0(\bar{D}^0)$, $D_s^{\pm}$
E687 [26]	γ	~ 220	$\sim 10^5$ $D^{\pm}$, $D^0(\bar{D}^0)$, $D_s^{\pm}$
E769 [27]	π	250	4×10^3 $D^{\pm}$, $D^0(\bar{D}^0)$, $D_s^{\pm}$
E791 [28]	π	500	$\sim 2 \times 10^5$ $D^{\pm}$, $D^0(\bar{D}^0)$, $D_s^{\pm}$
WA89 [29]	Σ^-	330	$\sim 10^4$ baryons

The E687 experiment [26] (Fig. 3) is the most prominent example of such an experiment. It was performed at Fermilab (USA) using a beam of photons. A beam of photons with an average energy of 220 GeV bombarded a beryllium target. Behind the target there was a vertex detector, which measured the coordinates of charged particles with high accuracy. The detector consisted of twelve planes of silicone microstrip detectors (SMD) grouped into four triplets. Each triplet of planes was used to determine the x and y coordinates of a particle. The accuracy with which the track coordinates were reconstructed amounted to 10 – 15 μm. The target and the vertex detector were followed by two magnets, M1 and M2, with oppositely directed magnetic fields, and five batteries of proportional wire chambers (P0 – P4). Such a system made it possible to measure the particle momenta with high accuracy. The type of particle was determined by three gas Cherenkov counters (C1 – C3). The ability of Cherenkov counters to yield information about the type of particle is based on the fact that charged particles moving with a velocity higher than the speed of light in the matter emit photons. The number of photons depends on the momentum and mass of the particle, with the result that by registering the photons we can determine the type of the charged particle. The Cherenkov counters are followed by a hadronic calorimeter (HC) and, finally, an identifier of muons (IM), shielded by iron. The hadronic calorimeter was used to measure the characteristics of charged pions. The design of this calorimeter is similar to that of the electromagnetic calorimeter, i.e. it consists of alternating metal and scintillator layers. Using it, one can find the total energy of the primary hadrons from the total energy released in the scintillator layers by numerous secondary hadrons produced as a result of the interactions of the primary particle in the metal layers. The hadronic calorimeter contains ten times more matter than the electromagnetic calorimeter, so that the larger amount of energy of

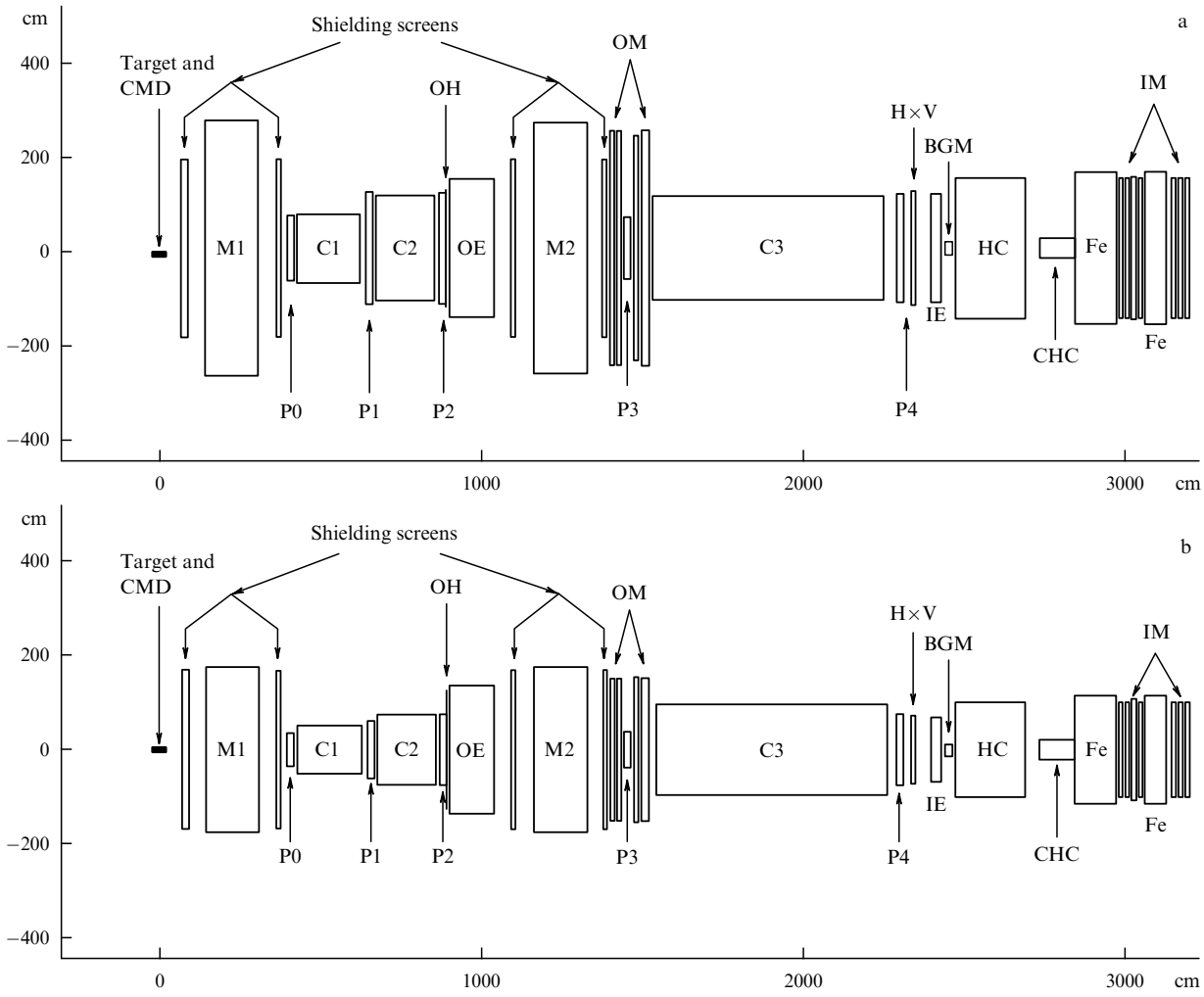

Figure 3. E687 detector: (a) side view; (b) top view. SMD, silicone microstrip detectors; M1 and M2, magnets; P0 – P4, proportional wire chambers; C1 – C3, gas Cherenkov counters; HC, hadronic calorimeter; and IM, identifier of muons.

the secondary hadrons is released inside the calorimeter. The most accurate results obtained to date for the lifetimes of charmed particles are those of the E687 experiment.

The E791 collaboration [28] achieved good results in studies of the properties of charmed particles. The experimental detector (Fig. 4) was located at the beam of 500-GeV π mesons at Fermilab. The target consisted of a 0.5-mm platinum foil and four 1.6-mm emerald foils positioned one after another and separated by a distance of 15 mm. The use of a target separated in this manner made it possible to substantially reduce the background from secondary interactions, i.e. to exclude events in which the decay products of a charmed particle undergo interactions in the matter of the same part of the target where the decay took place. To guarantee this, the candidates for charmed hadrons were selected in such a way that their decay would occur only in the air gap between the parts of the target, where the probability of secondary interactions occurring is negligible. The target was surrounded on both sides (along the beam) by silicon microstrip detectors and proportional wire chambers in order to be able to reconstruct, with high accuracy, the decay vertex and the tracks of the charged particles from charmed particle decay. The momenta of the decay products of the charmed particles were measured by a magnetic spectrometer, which consisted of two magnets and 35 planes of drift chambers positioned in front of and behind the magnets. Two threshold Cherenkov counters ensured the separation of kaon and pions in the 6 – 60 GeV/c momentum range.

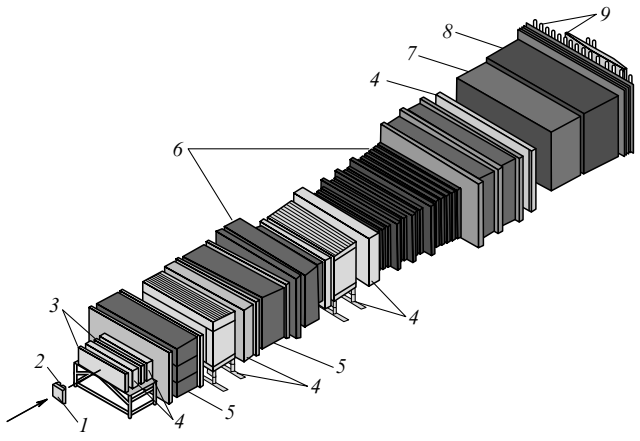

Figure 4. E791 detector: *1*, target; *2*, silicone microstrip detectors; *3*, proportional wire chambers; *4*, drift chambers; *5*, magnet; *6*, Cherenkov counters; *7*, electromagnetic calorimeter; *8*, hadronic calorimeter; and *9*, muon system.

The detectors described in this section contributed the most to the study of charmed particles.

3. Main processes contributing to the decay of charmed particles

The first experimental results in studies of charmed particles were described satisfactorily by the naive 'spectator' model [30], in which the heavy c quark is responsible for the decay of a charmed particle, while the light antiquark (or light quarks in the case of baryons) does not participate in the process, i.e. is the spectator. Figures 5a – c depict quark diagrams of spectator decays of charmed mesons. In the semileptonic decay of Fig. 5a, the transformation of the c quark into an s quark is accompanied by the emission of a virtual W boson, which decays to a lepton (l^+) and a neutrino (ν). The transformation of the $s\bar{q}$ pair into a strange meson is described by form-factors. Two hadron spectator diagrams are depicted in Fig. 5b and c, respectively. The only difference between diagrams 5b and 5a is that in 5b the W boson is transformed into a $u\bar{d}$ pair. Diagram 5c is often called a color suppressed diagram. Quarks are characterized not only by flavor (u, d, s, c, b, and t) but also by color. There are yellow, blue, and red quarks. However, the physically observable particles, the mesons and the baryons, are singlets in the color space (they are said to be colorless, or white). The color symmetry is strict, so that a colorless meson requires for its formation the interaction of a quark and antiquark of certain colors. In the case of diagram 5c, the $\bar{d}$ quark forming at the vertex of W decay is combined with the strange quark from the decay of the c quark. Therefore, it is natural to expect that the contribution of diagram 5c is suppressed in comparison to that of diagram 5b, where the u and $\bar{d}$ quarks constituting the pion are automatically of the correct color.

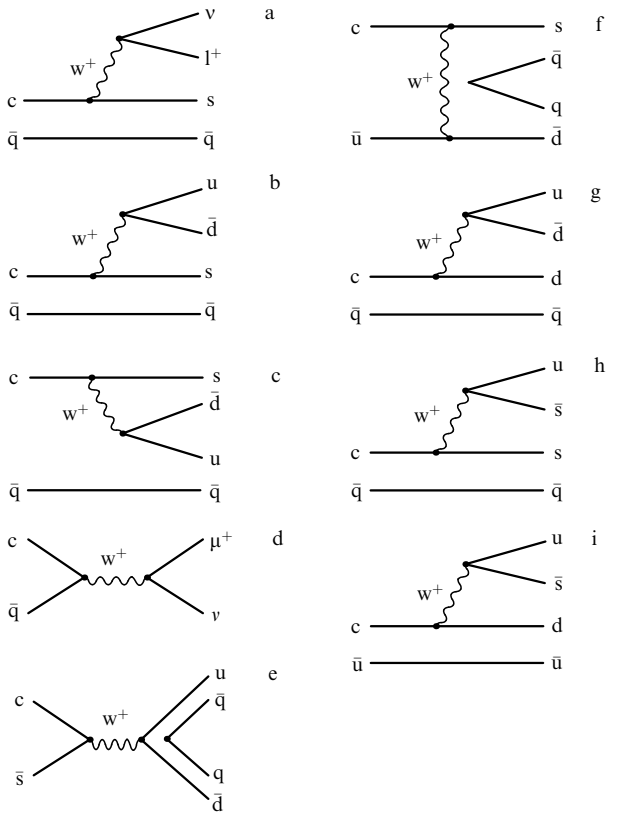

Figure 5. Meson diagrams.

Figures 5d – f depict the nonspectator quark diagrams contributing to the decay of charmed mesons. The annihilation diagram illustrating the leptonic decay $D \to \mu\nu$ is given in Fig. 5d. The contribution of the process described by the given diagram is suppressed. The suppression of the decay probability is due to the fact that for the spinless meson $M_{Q\bar{q}}$ the favorable helicity configuration in the decay $M_{Q\bar{q}} \to l^+\nu$ violates the law of angular momentum conservation. For massless particles the helicity is a strict quantum number, and a decay process with the production of finite-mass particles may occur with violation of the law of helicity conservation. The decay probability in this case is proportional to $f_D^2 m_l^2$, where f_D is the weak-decay constant for the D meson, and m_l is the mass of the respective lepton. Hence, the probability of leptonic decay of the D meson accompanied by muon (electron) production is low (negligible). Figures 5e and f depict two hadronic nonspectator diagrams: the W-annihilation diagram (Fig. 5e), and the W-exchange diagram (Fig. 5f). Diagram 5e contributes to such processes as, say, $D_s^+ \to \rho^0\pi^+$, while diagram 5f contributes to the decay process $D^0 \to \bar{K}^0\pi^0$, and its contribution is also suppressed due to violation of helicity conservation. Strong interaction partially reduces suppression in helicity in comparison to the leptonic decay, but the decay probability for the given diagram is still lower than it is for the spectator diagram.

In addition to diagrams describing the transformation of the c quark into the s quark, there are similar diagrams for the $c \to d$ transition (Fig. 5g). The probability of such processes is proportional to $\sin^2\theta_C \cos^2\theta_C$, where θ_C is the Cabibbo angle, and the respective processes are known as Cabibbo-suppressed (CS). Another type of diagram describing CS decays is diagram 5h, where the (us) pair is produced instead of the (ud) pair of Fig. 5b. Since the contribution of the spectator diagram describing Cabibbo-allowed (CA) decays is proportional to $\cos^4\theta_C$, the suppression factor for CS decays in relation to the corresponding allowed decays is equal to the ratio $\sin^2\theta_C/\cos^2\theta_C \sim 0.06$. Finally, Fig. 5i depicts the diagram of the doubly Cabibbo-suppressed (DCS) decay $D^0 \to K^+\pi^-$, whose probability is proportional to $\sin^4\theta_C$ and amounts to fractions of a percentage point of the probability of the CA decay $D^0 \to K^-\pi^+$.

Figures 6a – h depict the main quark diagrams for decays of charmed baryons: the spectator diagrams (the semileptonic diagram 6a and the hadronic diagrams 6b – d); the W exchange diagram 6e; and the CS and DCS diagrams 6f – h. In the case of baryons, the contribution of the 6e diagram is not suppressed in helicity, with the result that the corresponding processes occur with a probability that is comparable to that of spectator processes.

4. Spectroscopy of charmed hadrons

4.1 Ground states of charmed mesons

We will use the term 'ground state' for the $^1S_1$ and $^3S_1$ states of the quark – antiquark pair $c\bar{q}$, where $\bar{q}$ is a light antiquark ($\bar{u}, \bar{d}, \bar{s}$). The scalar mesons D^0 and D^+ (the ground states of the pairs $c\bar{u}$ and $c\bar{d}$) were discovered in 1976 in the MARK I experiment at the SLAC accelerator [10, 11]. Somewhat later the ground state of the $c\bar{s}$ pair was also discovered and was called the D_s meson. This charmed meson was first detected by the CLEO group in the $D_s^+ \to \phi\pi^+$ decay channel [31].

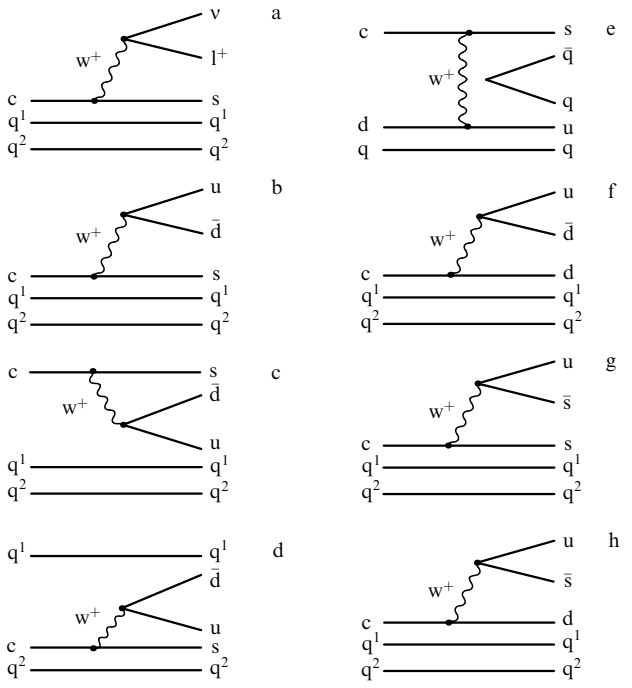

Figure 6. Baryon diagrams.

Soon after the discovery was corroborated by the TASSO [32] and ARGUS [33] groups, with the ARGUS group restoring this meson not only in the decay channel $D_s^+ \to \phi\pi^+$ but also in the channel $D_s^+ \to \phi\pi^+\pi^+\pi^-$. Measurements have already been made of many tens of decay channels of the D^0, D^+ and D_s^+ mesons. Exhaustive information about all detected decay channels can be found in the special publication *Review of Particle Physics* [34], in which the data is renewed every two years. Table 3 lists the branching fractions of the most characteristic D-meson decay modes.

The vector mesons D^{*+} and D^{*0} (the $^3S_1$ states of the pairs $c\bar{d}$ and $c\bar{u}$) were discovered in 1976 in the MARK I experiment [35]. The mesons D^{*+} and D^{*0} may decay due to the strong interaction, $D^{*+} \to D\pi$, and due to the electromagnetic interaction, $D^{*+} \to D^+\gamma$. The probability of electromagnetic decay is proportional to the magnetic moments of the quarks comprising the D meson. As a result of decay, the spin of the heavy c quark or the light antiquark contained in the D^* meson flips over. For the $D^{*0} \to D^0\gamma$ decay these two processes interfere constructively (one amplitude is added to the other), while for the $D^{*+} \to D^+\gamma$ decay the interference is destructive (one amplitude is subtracted from the other). Hence the probability of radiative decay of D^{*+} is much lower than that of D^{*0}. Measurements of the probability of electromagnetic decay are a good check of the validity of the standard model (SM) of electroweak interactions [2]. The decays $D^{*0} \to D^0\pi^0$ and $D^{*0} \to D^0\gamma$ were discovered soon after. Note that the probabilities of radiative and strong decays proved to be very close, although usually these probabilities differ by a factor of 10^4. The reason lies in the low energy release in the $D^{*0} \to D^0\pi^0$ decay (only several MeV), which leads to reduction of the probability of strong decay to the level of electromagnetic decay.

Only in 1997 was the decay $D^{*+} \to D^+\gamma$ detected by the CLEO group. The obtained value of the relative probability,

$$\mathrm{Br}(D^{*+} \to D^+\gamma) = (1.7 \pm 0.4 \pm 0.3)\% \; [37]\,,$$

agrees perfectly with the value predicted by the SM. The branching fractions for D^* meson decays are listed in Table 3.

For the $c\bar{s}$ system of quarks, the quark model predicts the existence of the vector state D_s^* similar to the D^* state for the $c\bar{q}$ system. The decay of D_s^* to the pseudoscalar meson D_s and a pion violates the law of isotopic spin conservation, since the initial state has zero isospin, while the final state has $I = 1$ due to the isospin of the pion. Nevertheless, decays violating the law of isotopic spin conservation are not forbidden completely. For instance, at the very dawn of studies of mesons with hidden charm the decay $\psi' \to J/\psi\pi^0$ was detected [38]. However, the probability of this decay is strongly suppressed. The increase in the branching fraction of the $D_s^{*+} \to D_s^+\pi^0$ decay can be explained by the fact that the main decay channel for D_s^{*+}, the radiative decay $D_s^{*+} \to D_s^+\gamma$, is also suppressed (similar to the decay $D^{*+} \to D^+\gamma$) in view of the destructive interference of the amplitudes of the two processes. The first to detect the radiative decay $D_s^{*+} \to D_s^+\gamma$ was the ARGUS group [39]. In 1995, the CLEO group discovered the decay $D_s^{*+} \to D_s^+\pi^0$ [40], whose probability was found to be 50 times lower than the radiative decay probability. Thus, all charmed mesons of the ground state are discovered. Table 3 lists the data on the main decay channels for these mesons.

Table 3. Ground-state mesons.

Meson	Mass, MeV/c^2	Main decay channels	Branching fraction, %
D^0	1864.1 ± 1.0	$K^-\pi^+\pi^0$	13.9 ± 0.9
		$K^-\pi^+\pi^-\pi^+$	7.6 ± 0.4
		$K^-\pi^+$	3.85 ± 0.09
		$K^-l^+\nu_l$	3.50 ± 0.17
D^+	1869.4 ± 0.5	$K^-\pi^+\pi^+$	9.0 ± 0.6
		$K^-\pi^+\pi^+\pi^0$	6.4 ± 1.1
		$\bar{K}^0\pi^+\pi^+\pi^-$	7.0 ± 0.9
		$\bar{K}^0l^+\nu_l$	6.8 ± 0.8
D_s^+	1969.0 ± 1.4	$K^+K^-\pi^+$	4.4 ± 1.2
		$\phi\pi^+$	3.6 ± 0.9
		$K^+\bar{K}^0$	3.6 ± 1.1
		$\phi l^+\nu_l$	2.0 ± 0.5
D^{*0}	2006.7 ± 0.5	$D^0\pi^0$	61.9 ± 2.9
		$D^0\gamma$	38.1 ± 2.9
D^{*+}	2010.0 ± 0.5	$D^0\pi^+$	68.1 ± 1.4
		$D^+\pi^0$	30.6 ± 2.5
		$D^+\gamma$	1.7 ± 0.5
D^{*+}	2112.9 ± 1.5	$D_s^+\gamma$	94.2 ± 2.5
		$D_s^+\pi^0$	5.8 ± 2.5

4.2 Excited states of charmed mesons

In 1985, the ARGUS group discovered a meson with a mass of about 2420 MeV/c^2. The meson was found to decay to $D^{*+}\pi^-$ [43] and proved to be an excited state of a charmed meson with orbital angular momentum $L = 1$.

The discovery of the first excited state of a charmed meson was the cause of a lot of experimental work and also forced the theoreticians to revise their previous ideas about the properties of excited states of charmed mesons. The existence of four $c\bar{q}$ states with $L = 1$ is predicted: a triplet of states corresponding to the sum of the orbital angular momentum $L = 1$ and the spin $s = 1$ of the $c\bar{q}$ system, and a singlet

[2] The standard model of electroweak interactions was developed by Glashow, Salam, and Weinberg to describe the weak and electromagnetic interactions of elementary particles [36].

corresponding to the sum of $L = 1$ and $s = 0$ of the $c\bar{q}$ system. The spin symmetry of heavy quarks presupposes that the properties of P-wave mesons ($L = 1$) are determined primarily by the total angular momentum of the light quark: $j_q = L + s_q$, where s_q is the spin of the light quark. Then, in the limit of an infinitely heavy charmed quark, all four states (the triplet and the singlet) form two doublets with $j_q = 1/2$ and $j_q = 3/2$, respectively. The P-wave mesons decay primarily to $D^{(*)} + \pi$ and $D^{(*)} + K$ for D^{**} and D_s^{**}, respectively. In this case the laws of conservation of angular momentum and parity determine, for each state, the allowed decay channels and the allowed wave states [41, 42]. The members of the doublet $j_q = 1/2$ split in the S wave and, hence, it is expected that the width of these states is of order 100 – 200 MeV/c^2. The doublet $j_q = 3/2$ can split only by passing through a D wave, so that it is expected that these states are narrow (of order 10 – 20 MeV/c^2). All six expected narrow states ($j_q = 3/2$) were detected in two experiments, ARGUS [43, 44] and CLEO [45]. Some of these states were also detected in fixed-target experiments [46, 47] and, in recent years, in LEP experiments [48]. Table 4 lists the main characteristics of excited states of charmed mesons with $L = 1$.

Table 4. Main characteristics of mesons with $L = 1$.

Meson	Mass, MeV/c^2	Width, MeV/c^2	Decay channels
D_1^0	2422.2 ± 1.8	$18.9^{+4.6}_{-3.5}$	$D^*\pi$
D_2^{*0}	2458.9 ± 2.0	23 ± 5	$D^*\pi$, $D\pi$
D_1^+	2427 ± 5	28 ± 8	$D^*\pi$
D_2^{*+}	2459 ± 4	25^{+8}_{-7}	$D^*\pi$, $D\pi$
D_{s1}^{*+}	2535.35 ± 0.34	< 2.3 (90 % CL)	D^*K
D_{s2}^{*+}	2573.5 ± 1.7	15^{+5}_{-4}	D^*K, DK

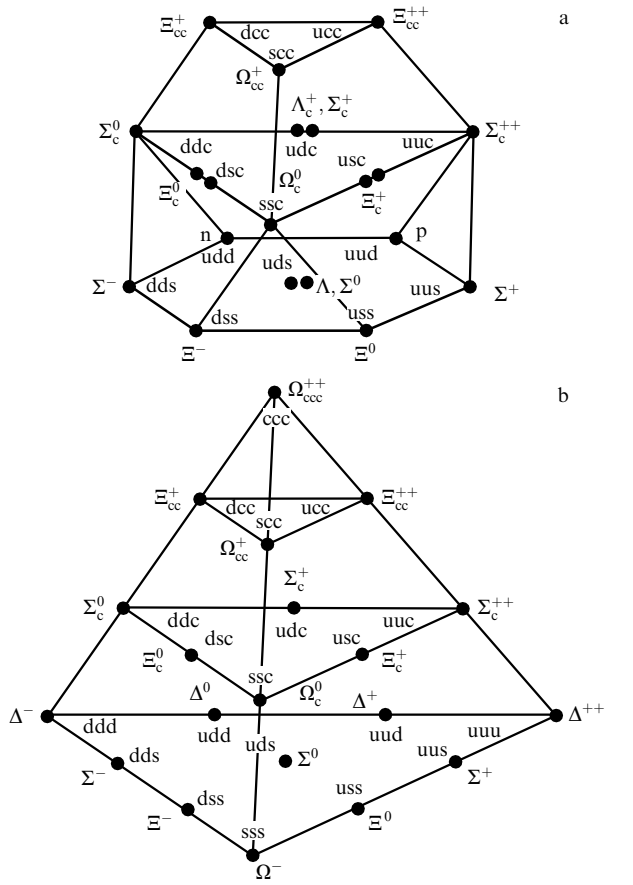

Figure 7. (a) Baryon multiplet with $J^P = 1/2^+$; (b) baryon multiplet with $J^P = 3/2^+$.

4.3 Ground states of charmed baryons

The ground states of charmed baryons constitute an integral part of two SU(4) multiplets in which each baryon contains three quarks of one of the four flavors (u, d, s, c). The first multiplet contains baryons with $J^P = 1/2^+$ (Fig. 7a) and the second, baryons with $J^P = 3/2^+$ (Fig. 7b). Let us focus on the multiplet with $J^P = 1/2^+$, whose middle level incorporates states with one c quark. This multiplet incorporates the singlet Λ_c^+ with the quark composition (cud); the triplet of states Σ_c^0, Σ_c^+, and Σ_c^{++} with the quark composition (cdd), (cud), and (cuu); two isotopic doublets Ξ_c^0, Ξ_c^+ and $\Xi_c^{0\prime}$, $\Xi_c^{+\prime}$ (cds and cus); and the isosinglet Ω_c^0 (css). The nine states are combined into two SU(3)-multiplets: a triplet of states asymmetric with respect to the permutation of a pair of noncharmed quarks ($\bar{3}$) incorporating Λ_c^+, Ξ_c^0, and Ξ_c^+, and a sextet of states symmetric with respect to the permutation of a pair of noncharmed quark (6) incorporating Σ_c^0, Σ_c^+, Σ_c^{++}, $\Xi_c^{0\prime}$, $\Xi_c^{+\prime}$, and Ω_c^0. Since the difference in masses $[m(\Xi_c') - m(\Xi_c)]$ is smaller than the pion mass, Ξ_c' decays to Ξ_c and emits a photon in the process. Indication of such a decay of Ξ_c' were found in the CLEO experiment [49]. All the other charmed baryon states $J^P = 1/2^+$ with one c quark have been discovered. In particular, while the Λ_c^+ and Σ_c states have been known for more than ten years and detailed information about these states has been extracted in many experiments [34], the situation with Ω_c^0 is still unclear. In 1985, the WA62 group [50] discovered three events in the distribution in the invariant mass of $\Xi^-K^-\pi^+\pi^+$ in the mass range 2740 ± 20 MeV/c^2. But only after almost ten years did the ARGUS group [51] discovered 12 ± 5 and 7 ± 3 events in the decay channels $\Omega_c^0 \to \Xi^-K^-\pi^+\pi^+$ and $\Omega_c^0 \to \Omega^-\pi^-\pi^+\pi^+$, respectively. Indications of the decay $\Omega_c^0 \to \Omega^-\pi^+$ were found in the E687 experiment [52]. Also in this experiment several tens of events were discovered in which Ω_c^0 decayed to $\Sigma^+K^-K^-\pi^+$ and $\Omega^-\pi^+$ [53]. Finally, the WA89 collaboration obtained preliminary results on the reconstruction of Ω_c^0 in seven different decay channels with the statistics of about 200 events [54]. However, the values of the masses of states reconstructed in different experiments vary from 2695 ± 4 to 2723 ± 7 MeV/c^2 with an average value of 2704 ± 2.5 MeV/c^2. Neither has Ω_c^0 been detected in the CLEO experiment, which so far has the largest number of reconstructed charmed particles to its credit. Table 5 lists the characteristics of the ground states of charmed baryons. The baryons Λ_c^+, Ξ_c^0, Ξ_c^+, and Ω_c^0 decay due to the weak interaction, the triplet of states Σ_c^0, Σ_c^+, and Σ_c^{++} decay due to the strong interaction, and the

Table 5. Charmed baryons with $J^P = 1/2^+$.

Baryon	Mass, MeV/c^2	Main decay channels
Λ_c^+	2284.9 ± 0.6	$pK^-\pi^+$
Σ_c^{++}	2453.1 ± 0.6	$\Lambda_c^+\pi^+$
Σ_c^+	2453.8 ± 0.9	$\Lambda_c^+\pi^0$
Σ_c^0	2452.4 ± 0.7	$\Lambda_c^+\pi^-$
Ξ_c^+	2465.4 ± 1.6	$\Lambda K^-\pi^+\pi^+$
Ξ_c^0	2470.4 ± 2.0	$\Xi^-\pi^+\pi^+\pi^-$
$\Xi_c'^+$	2573.7 ± 3.3	$\Xi^+\gamma$
$\Xi_c'^0$	2577.4 ± 3.5	$\Xi^0\gamma$
Ω_c^0	2704 ± 4	$\Sigma^+K^-K^-\pi^+$

doublet of states $\Xi_c^{0\prime}$ and $\Xi_c^{+\prime}$ decay due to the electromagnetic interaction.

The first experimental data on charmed baryon states with $J^P = 3/2^+$ appeared in 1993 after an experiment at the Serpukhov proton synchrotron in which the interaction of neutrinos in a hydrogen chamber was studied. The experimenters detected six events in which the invariant mass of $\Lambda_c^+\pi^+$ combinations amounted to $2530 \pm 5 \pm 5$ MeV/c^2 [55]. According to their estimates, the possible background does not exceed one event. The detected state was interpreted as the baryon Σ_c^{*++} with $J^P = 3/2^+$. Over the last two years, thanks to the CLEO collaboration, the existence of this state has been corroborated and three more states of charmed baryons belonging to the multiplet with $J^P = 3/2^+$, namely, Ξ_c^{*0}, Ξ_c^{*+}, and Σ_c^{*0}, have been observed [56]. Only two states out of the six states of the multiplet with $J^P = 3/2^+$ have yet to be discovered: Σ_c^{*+} and Ω_c^{*0}. It is expected that the main decay channels for these baryons are $\Sigma_c^{*+} \to \Lambda_c^+\pi^0$ and $\Omega_c^{*0} \to \Omega_c^0\gamma$, respectively. Both channels contain neutral particles, which hinder the detection of these baryons.

The main characteristics of the detected states are listed in Table 6, where the values of the difference of masses of the excited and the respective ground states are also given. It is this mass difference that is calculated in all theoretical models. The same quantity is determined in experiments to a high accuracy, since it does not contain systematic errors related to finding the mass of the ground state.

Table 6. Charmed baryons with $J^P = 3/2^+$ detected in experiments.

Baryon	Mass, MeV/c^2	Main decay channel	Δm, MeV/c^2
Σ_c^{*++}	2519.4 ± 1.5	$\Lambda_c^+\pi^+$	$234.5 \pm 1.1 \pm 0.8$
Σ_c^{*0}	2522.0 ± 1.4	$\Lambda_c^+\pi^-$	$232.6 \pm 1.0 \pm 0.8$
Ξ_c^{*+}	2644.6 ± 2.3	$\Xi_c^0\pi^+$	$174.3 \pm 0.5 \pm 1.0$
Ξ_c^{*0}	2642.8 ± 2.2	$\Xi_c^+\pi^-$	$178.2 \pm 0.5 \pm 1.0$

4.4 Excited states of charmed baryons

An excited state of a charmed baryon was first discovered in the ARGUS experiment in 1993 [57]. The baryon was reconstructed in the $\Lambda_c^+\pi^+\pi^-$ decay channel. The two light quarks in the baryon have an orbital angular momentum equal to unity with respect to the heavy (charmed) quark. This scheme presupposes the existence of a doublet of excited charmed baryons with the quantum numbers $J^P = 1/2^-$ and $J^P = 3/2^-$, and that the observed charmed baryon is a baryon with $J^P = 3/2^-$. Today this state is denoted by Λ_{c1}^+, where the subscript 'one' stands for the orbital angular momentum of the light quarks. Later the existence of this excited state was corroborated in other experiments [58], and also the partner Λ_{c1}^+ in the doublet was discovered. In 1997, the CLEO collaboration discovered a similar orbital excited state in the Ξ_c^+ sector [49]. Table 7 lists the main characteristics of the different excited states.

Table 7. Excited states of charmed baryons detected in experiments.

Baryon	Mass, MeV/c^2	Main decay channel
$\Lambda_{c1}(1/2)^+$	2593.6 ± 1.0	$\Sigma_c\pi$
$\Lambda_{c1}(3/2)^+$	2626.4 ± 0.9	$\Lambda_c^+\pi^+\pi^-$
$\Xi_{c1}(3/2)^+$	2815.0 ± 1.9	$\Xi_c^*\pi^+$

5. Lifetimes of charmed particles

The lifetimes of all the known charmed hadrons that decay due to the weak interaction have been measured. The meson lifetimes are known to within 2–3%, while the accuracy of measuring the baryon lifetimes varies from 5.5% for Λ_c^+ to approximately 30% for Ω_c^0. The modern experimental situation is reflected in Table 8.

Table 8. Lifetimes of charmed particles in picoseconds.

Hadron	World mean [34]	Accuracy, %	E687 [59]
D^+	1.057 ± 0.015	1.4	$1.048 \pm 0.015 \pm 0.011$
D^0	0.415 ± 0.004	1.0	$0.413 \pm 0.004 \pm 0.003$
D_s^+	0.467 ± 0.017	3.6	$0.475 \pm 0.020 \pm 0.007$
Λ_c^+	$0.200^{+0.011}_{-0.010}$	5.5	$0.215 \pm 0.016 \pm 0.008$
Ξ_c^0	$0.098^{+0.023}_{-0.015}$	23	$0.101^{+0.025}_{-0.017} \pm 0.005$
Ξ_c^+	$0.34^{+0.06}_{-0.04}$	16	$0.41^{+0.11}_{-0.08} \pm 0.02$
Ω_c^0	$0.063^{+0.019}_{-0.020}$	30	$0.089^{+0.027}_{-0.020} \pm 0.028$

The main contribution to the existing values (averaged over the results of all the measurements) of the lifetimes of charmed hadrons was provided by the E687 collaboration [59]. As noted earlier, it is much easier to measure the lifetimes of particles in fixed-target experiments. Electron–positron colliders were used only to measure the lifetimes of D mesons, and up to 1998 the best of these measurements in the ARGUS experiment [60] [3] was five to seven times less accurate than those conducted by the E687 collaboration [59].

In 1995, two collaborations announced the results of measurements of the lifetime of Ω_c^0, the shortest-lived charmed baryon, which decays due to the weak interaction. The E687 experiment used Ω_c^0 baryons, which were reconstructed completely from the decay channel $\Omega_c^0 \to \Sigma^+K^-K^-\pi^+$ (in turn, Σ^+ was reconstructed from the decays to $n\pi$ and $p\pi^0$). The measured value of the lifetime, $\tau_{\Omega_c} = 0.089^{+0.027}_{-0.020} \pm 0.028$ ps [62] was so small that it was comparable to the limit of accuracy achievable by modern detectors. Lifetime measurements required using a precision detector for measuring the decay vertex for the Ω_c^0 baryon and employing complicated mathematics in extracting the lifetimes from the results of measurements. With such short lifetimes it is necessary to thoroughly investigate all possible sources of systematic errors related to the nonuniformity of the detectors and the precision with which various parts of the detector operate.

At almost the same time the results of the WA89 collaboration of measurements of the lifetime of Ω_c^0 were published [63]. To measure the lifetime, the researchers used Ω_c^0 baryons reconstructed from the $\Omega^-\pi^+\pi^-\pi^+$ and $\Xi^-K^-\pi^+\pi^+$ decay channels. The lifetime of the Ω_c^0 baryon averaged over the results of measurements for the two decay channels, $\tau_{\Omega_c} = 0.055^{+0,013}_{-0,011} \pm 0.02$ ps [63], coincided, to within experimental error with the E687 result.

Measurements of the lifetime of the Ω_c^0 baryon made it possible to find the relationship that exists between the

[3] Preliminary data obtained by the CLEO collaboration appeared in 1998. Using a new vertex detector, the researchers measure the D-meson lifetimes with an accuracy comparable to that of the E687 measurements: $\tau_{D^0} = 0.403 \pm 0.009^{+0.007}_{-0.011}$ ps, $\tau_{D^+} = 1.034 \pm 0.033^{+0.033}_{-0.038}$ ps, and $\tau_{D_s^+} = 0.475 \pm 0.024 \pm 0.025$ ps [61].

lifetimes of all the charmed hadrons that decay due to the weak interaction

$$\tau(\Omega_c^0) < \tau(\Xi_c^0) < \tau(\Lambda_c^+) < \tau(\Xi_c^+) < \tau(D^0) < \tau(D_s^+) < \tau(D^+)\,.$$

In the simplest variant of the spectator mode of the decay of heavy quarks (c and b quarks), the light quark has little effect on the decay, whose probability is completely determined by the characteristics of the heavy quark. Within this model, it is natural to conclude that the lifetimes of all the charmed hadrons are approximately the same. This, however, contradicts the experimental results listed in Table 8, according to which the lifetime of the longest-lived charmed hadron D^+ is greater than the lifetime of the Ω_c^0 baryon by a factor of ten, while the lifetimes of the charged and neutral D mesons differ by a factor of 2.5. These experimental facts forced theoreticians to focus on the relationship between the lifetimes of charmed particles. The difference in the lifetimes of the charged and neutral D mesons is related to the difference in the probabilities of hadronic decays, and the primary reasons for this are as follows [64]:

1. The decays of D^+, in contrast to the decays of D^0, lead to final states containing two antiquarks of the same flavor, $\bar{d}$. As a result of the interference of the various quark diagrams (and in the case of the D^+ meson this interference is destructive), the decay probability decreases. Hence the lifetime of D^+ increases in comparison to the lifetime of D^0.

2. The W-exchange diagram (Fig. 5f) contributes only to the decays of D^0 and, therefore, only increases the difference between the lifetimes of D^+ and D^0. As noted earlier, such processes are suppressed due to the violation of the helicity conservation law. However, processes of the type depicted in Fig. 8, where the light antiquark emits a bremsstrahlung gluon, can reduce the suppression and substantially enhance the contribution of the W-exchange diagram.

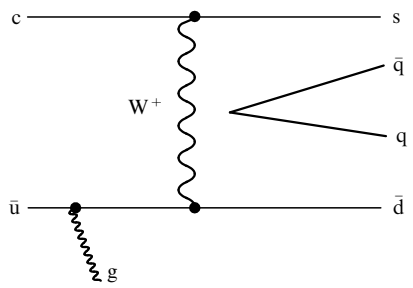

Figure 8. Diagram of a W-meson exchange with emission of a gluon.

Allowing for these two causes leads to the following qualitative estimate of the lifetime ratio:

$$\frac{\tau(D^+)}{\tau(D^0)} \approx 1 + \left(\frac{f_D}{200\ \text{MeV}}\right)^2 \sim 2\,,$$

i.e. agrees with the experimental result with an accuracy of 25%. Higher-order contributions must be taken into account if we want better agreement between theory and experiment [64].

The value of the lifetime ratio, $\tau(D_s^+)/\tau(D^0) = 1.12 \pm 0.04$ is determined by several factors.

The lifetime $\tau(D_s^+)$ increases by three to five percent for each of the following reasons [64]:

(1) violation of the SU(3) symmetry leads to corrections that increase the lifetime of D_s^+;

(2) destructive interference for CS decays of D_s^+ decreases the decay probability for D_s^+.

The additional decay channel $D_s^+ \to \tau^+\nu$, which is absent in the case of neutral D^0, decreases this difference by three percent. The total effect of allowing for all three contributions leads to a lifetime ratio $\tau(D_s^+)/\tau(D^0) \approx 1.03-1.07$. The remaining difference can be explained by the contribution of annihilation diagrams to the decays of D^0. A comparison of the experimental value of the ratio with the values predicted by theory suggests that the contribution of the annihilation diagrams provides 10 to 20% of the value of the lifetime ratio for charmed mesons.

The following effects contribute the most to the lifetimes of charmed baryons [64]:

(1) just as in the case of mesons, there is destructive interference between diagrams 6b and 6d when the light spectator quark q^1 is a u quark (Λ_c^+, Ξ_c^+);

(2) in the case of spectator s-quark, between diagrams 6c and 6d there is constructive (amplifying) interference (Ξ_c^+, Ξ_c^0); and

(3) as noted earlier, for baryons the exchange diagram 6e can contribute considerably when the baryon contains a d quark (Λ_c^+, Ξ_c^0).

With allowance for the different influence of these effects on the lifetimes of charmed baryons, the following theoretical predictions were made:

$$\tau(\Omega_c^0) \approx \tau(\Xi_c^0) < \tau(\Lambda_c^+) < \tau(\Xi_c^+)\ [65]\,,$$
$$\tau(\Omega_c^0) < \tau(\Xi_c^0) < \tau(\Lambda_c^+) \approx \tau(\Xi_c^+)\ [66]\,,$$
$$\tau(\Omega_c^0) < \tau(\Xi_c^0) < \tau(\Lambda_c^+) < \tau(\Xi_c^+)\ [67]\,.$$

All these predictions provide only a qualitative description of the lifetime ratio.

Today the accuracy achieved in experiments is much better than that achieved in the theory. While explaining the value of the lifetime ratio $\tau(D^+)/\tau(D^0)$ qualitatively, the theory is unable to reproduce this value quantitatively with an accuracy of two to three percent. Neither do the existing theoretical models explain the experimentally established relationship between the lifetimes of charmed baryons, namely, $\tau(\Omega_c^0) < \tau(\Xi_c^0) < \tau(\Lambda_c^+) < \tau(\Xi_c^+)$.

6. Leptonic decays of charmed hadrons

The purely leptonic decay of charmed mesons is the simplest for theoretical description. In this case the effect of the strong interaction can be described by using a single parameter, known as the decay constant. In the most general form, the matrix element for the decay of a charged pseudoscalar meson $M_{Q\bar{q}}$ with the production of a lepton (l) and a neutrino (ν) is described by the following expression [68]:

$$\Gamma(M_{Q\bar{q}} \to l\nu) = \frac{G_F^2}{8\pi}|V_{qQ}|^2 f_M^2 M m_l^2 \left(1 - \frac{m_l^2}{M^2}\right)^2\,,$$

where G_F is the weak interaction constant, f_M is the decay constant, V_{qQ} is the element of the Kobayashi – Maskawa matrix [69], and m_l and M are the masses of the lepton and the meson $M_{Q\bar{q}}$. The decay constant f_M describes the probability of quark annihilation. In the limit of an infinitely heavy quark, the decay constant f_M is given by the nonrelativistic

formula $f_M^2 = 12|\psi(0)|^2/M$, where $\psi(0)$ is the wave function of the light antiquark $\bar{q}$ and the heavy quark Q when the distance between the quarks is zero. The factor m_l^2 emerges because of suppression caused by violation of the helicity conservation law (see Section 3). This suppression leads to a situation in which the probability of decay to lighter leptons is much smaller than the probability of decay to a heavy lepton.

According to theoretical predictions [70], the value of the decay constant f_D lies in 170-to-240-MeV range, while f_{D_s} is expected to be larger by 10%. Measuring the decay constants f_D and f_{D_s} is important not only from the standpoint of increasing our knowledge about charmed particles but also because it provides a means for making reliable estimates for the decay constant of the B meson, f_B. It is still practically impossible to extract the value of f_B from the results of experimental measurements of leptonic decays of B mesons, since the branching fractions of the leptonic decays of B mesons are small even in comparison to those of leptonic decays of D mesons. Table 9 lists the theoretical estimates of the widths and branching fractions of leptonic decays for D^+ and D_s^+ mesons taken from Ref. [68].

Table 9. Theoretical estimates of the widths and relative probabilities of leptonic decays of D^+ and D_s^+.

Decay channel	Decay width, s^{-1}	Branching fraction
$D^+ \to e^+\nu_e$	7.1×10^3	7.5×10^{-9}
$D^+ \to \mu^+\nu_\mu$	3.0×10^8	3.2×10^{-4}
$D^+ \to \tau^+\nu_\tau$	6.8×10^8	7.2×10^{-4}
$D_s^+ \to e^+\nu_e$	1.6×10^5	7.5×10^{-8}
$D_s^+ \to \mu^+\nu_\mu$	6.8×10^9	3.2×10^{-3}
$D_s^+ \to \tau^+\nu_\tau$	6.1×10^{10}	2.9×10^{-2}

The decays $D_s^+ \to \mu^+\nu_\mu$ and $D_s^+ \to \tau^+\nu_\tau$ have been detected in several experiments. The first indication that the decay $D_s^+ \to \mu^+\nu$ exists was obtained at CERN in 1992 in the WA75 experiment with a fixed target [71]. The distribution in the transverse component of the muon momentum p_t^μ exhibited an excess of events in the region $p_t^\mu > 0.9$ GeV/c that could not be explained either by the $D^+ \to \mu^+\nu$ decay or by semileptonic decays of D_s^+.

The next year the CLEO group measured the probability of the decay $D_s^+ \to \mu^+\nu$ in relation to the decay $D_s^+ \to \phi\pi^+$ [72]. In their experiment the researchers studied $\mu\gamma$ combinations formed as a result of the following chain of decays: $D_s^{*+} \to D_s^+\gamma$, $D_s^+ \to \mu^+\nu$. The neutrino–matter interaction cross section is negligible, so it is impossible to detect neutrinos in this experiment. Nevertheless, the detector is hermetic enough that by using the information about all the particles registered in an event it is possible to determine the characteristics of the neutrino. The neutrino momentum was estimated by the law of momentum conservation for the particles in the event, while the neutrino energy was estimated by the energy and momentum lost in the hemisphere where the muon was detected. Figure 9 depicts the distribution for the mass difference $\Delta M = m(\mu\nu_\mu\gamma) - m(\mu\nu_\mu)$ obtained in the experiment of Acosta et al. [72]. In the events in which the decay chain $D_s^{*+} \to D_s^+\gamma$, $D_s^+ \to \mu^+\nu$ was present, a peak is expected in the mass-difference distribution at $m(D_s^*) - m(D_s) \approx 140$ MeV/c^2. To estimate the level of the background from random combinations of μ and γ, a similar distribution for e and γ was used. Since the probability of the decay $D_s^+ \to e^+\nu$ is negligible compared to the probability of the decay $D_s^+ \to \mu^+\nu$, the distribution of the $e\gamma$ combinations, after correction for the difference in the probabilities of misidentification of a pion as a muon and a pion as an electron, can be used to estimate the background. In Fig. 9 the distribution of $e\gamma$ combinations is depicted by the dashed line and the hatched histogram gives an information about the extent to which the contribution of the misidentification of particles as muons is larger than the contribution of the misidentification of particles as electrons. As a result of subtracting the electron distribution from the muon distribution and taking into account the difference in misidentification rates, there was found to be an excess amounting to 38 ± 10 events. The excess appeared because of the following chain of decays $D_s^{*+} \to D_s^+\gamma$, $D_s^+ \to \mu^+\nu$. This corresponds to the following value for the probability ratio:

$$\frac{\mathrm{Br}(D_s^+ \to \mu^+\nu_\mu)}{\mathrm{Br}(D_s^+ \to \phi\pi^+)} = 0.245 \pm 0.052 \pm 0.074\,.$$

This relationship was used to determine the value of the decay constant f_{D_s}:

$$f_{D_s} = (344 \pm 37 \pm 52)\sqrt{\frac{\mathrm{Br}(D_s^+ \to \phi\pi^+)}{0.037}}\ \mathrm{MeV}\,.$$

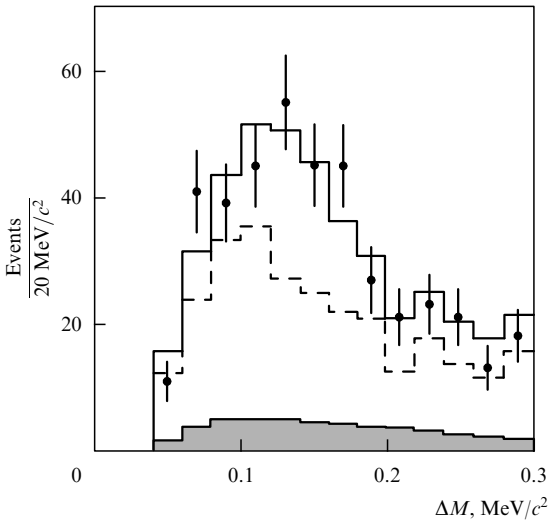

Figure 9. Distributions of D_s^{*+} in the mass difference for muon data (solid line) and electron data (dashed line) and for the excess of the misidentification of particles as muons over the misidentification of particles as electrons (hatched area).

In 1997, the CLEO group significantly improved the accuracy of measuring the decay constant f_{D_s} (Table 10). To obtain the new result the researchers used an improved algorithm of analysis and a modified estimate of the probability of misidentification of a particle as a lepton. They also significantly reduced systematic errors by gathering experience in operating the detector.

Purely leptonic decays were also studied in the E653 [74] and the BES [75] experiments. To detect the decay $D_s^+ \to \mu^+\nu$, the E653 collaboration used the strong points of the emulsion experiment [74]. The vertex of the interaction, as a result of which charmed particles were produced, was identified visually. The search area was determined from the readings of a vertex silicone detector. Due to visual analysis, the efficiency of finding the interaction vertex was extremely high. The number of selected purely leptonic decays $D_s^+ \to \mu^+\nu_\mu$ was $23.2 \pm 6.0^{+1.0}_{-0.9}$. Using the $18.7 \pm 4.9^{+0.4}_{-0.7}$

Table 10. Experimental values of the decay constants of D mesons, f_D and f_{D_s}. The values of the pion and kaon decay constants f_π and f_K averaged over all measurements are given for the sake of comparison.

Decay channel	Experiment	Value, MeV
f_{D_s}	WA75 [71]	$225 \pm 45 \pm 20 \pm 41$
f_{D_s}	CLEO II [72]	$344 \pm 37 \pm 52$
f_{D_s}	CLEO II [73]	$280 \pm 17 \pm 25 \pm 34$
f_{D_s}	E653 [74]	$194 \pm 35 \pm 20 \pm 14$
f_{D_s}	BES [75]	$430^{+150}_{-130} \pm 40$
f_{D_s}	L3 [77]	$309 \pm 58 \pm 33 \pm 38$
f_D	MARK III [78]	< 290
f_D	BES [79]	$300^{+180+80}_{-150-40}$
f_π	PDG [34]	130.7 ± 0.4
f_K	PDG [34]	159.8 ± 1.5

events of the decay $D_s^+ \to \phi\mu^+\nu_\mu$ selected earlier in the same experiment [76], the researchers found that

$$\frac{\mathrm{Br}(D_s^+ \to \mu^+\nu_\mu)}{\mathrm{Br}(D_s^+ \to \phi\mu^+\nu_\mu)} = 0.16 \pm 0.06 \pm 0.03\,.$$

The BES collaboration completely reconstructed three events in which one of the mesons (D_s^+ or D_s^-) decayed to a lepton and a neutrino. After normalizing to the number of events in which at least one D_s is fully reconstructed, the researchers arrived at the following expression for the decay constant:

$$f_{D_s} = (430^{+150}_{-130} \pm 40)\ \mathrm{MeV}\,.$$

The principal merit of this result lies in the fact that, in contrast to other results, obtaining it did not require knowing the branching fraction of the decay $D_s \to \phi\pi^+$ (this knowledge introduces an additional error into the final result). In the future, when the accuracy of the measurements will not be limited by the statistics but will depend on the values of the systematic errors, the method used in the BES experiment will undoubtedly be preferable. Finally, the decay $D_s^+ \to \tau^+\nu$ was also studied in the L3 experiment at CERN [77]. The experimenters used a method similar to that employed earlier by the CLEO group in studies of the decay $D_s^+ \to \mu^+\nu$. The signal was observed in the distribution in the invariant mass $M(\gamma D_s^+)$, where γ and D_s^+ are produced as a result of the decay of D_s^{*+} through the following channel: $D_s^{*+} \to D_s^+\gamma$, $D_s^+ \to \tau^+\nu$. Table 10 lists the values of the decay constant f_{D_s} extracted from the above experiments.

Information about the decay $D^+ \to \mu^+\nu$ is much more scant. The MARK III collaboration [78] has obtained an upper limit on the branching fraction of the decay $D^+ \to \mu^+\nu$ and the corresponding upper limit on the decay constant f_D. A search for leptonic decays of D^+ in the reaction $e^+e^- \to D^{*+}D^-$ was conducted by the BES group [79] with a center-of-mass energy equals to 4.3 GeV. Only one event was detected in which D^- decayed by the $D^- \to \mu^-\nu_\mu$ channel and D^{*+} decayed according to the following scheme: $D^{*+} \to \pi^+D^0$, $D^0 \to K^-\pi^+$. Bai et al. [79] arrived at an estimate of the branching fraction, $\mathrm{Br}(D^- \to \mu^-\nu) = 0.08^{+0.16+0.05}_{-0.05-0.02}\%$ and the corresponding upper limit on the decay constant f_D, whose values are listed in Table 10. The values of the pion and kaon decay constants f_π and f_K averaged over all measurements are listed in Table 10 for the sake of comparison.

7. Semileptonic decays of charmed hadrons

7.1 Semileptonic decays of charmed mesons

The interest in inclusive semileptonic decays of D mesons has been fueled by the unexpectedly large difference in the lifetimes of D^0 and D^+. Until recently the most exact measurements of the branching fractions of inclusive semileptonic decays were the data of the MARK III collaboration, obtained more than a decade ago [80].The experimenters studied more than 5×10^4 $D\bar{D}$ pairs produced as a result of the decay of the $\psi(3770)$ resonance. The events selected were those in which one of the D mesons was completely reconstructed. There were about 1700 events for D^+D^- and approximately twice as many events for $D^0\bar{D}^0$. The number of electrons emitted in the direction opposite to that of the motion of the reconstructed D meson was then counted and the result was divided by the total number of partially reconstructed events. What was obtained was the relative probability of the inclusive semileptonic decay. This led to the following values of the branching fractions of semileptonic decays of D mesons:

$$\mathrm{Br}(D^+ \to Xe^+\nu_e) = (17.0 \pm 1.9 \pm 0.7)\%\,,$$
$$\mathrm{Br}(D^0 \to Xe^+\nu) = (7.5 \pm 1.1 \pm 0.4)\%$$

and the corresponding ratio:

$$\frac{\mathrm{Br}(D^+ \to Xe^+\nu_e)}{\mathrm{Br}(D^0 \to Xe^+\nu_e)} = 2.3^{+0.5}_{-0.4} \pm 0.1$$

(X stands for the hadrons produced as a result of semileptonic decay).

In recent years the branching fraction of the decay $D^0 \to Xl^+\nu$ was measured by three experiments. In 1994, the E653 collaboration established (see Ref. [81]) that

$$\frac{\Gamma(D^0 \to K^-\mu^+\nu_\mu)}{\Gamma(D^0 \to X\mu^+\nu_\mu)} = 0.472 \pm 0.051 \pm 0.040\,.$$

This ratio can be used to extract the value of the branching fraction of the inclusive semileptonic decay by employing the averaged value of $\mathrm{Br}(D^0 \to K^-\mu^+\nu_\mu)$ [34]:

$$\mathrm{Br}(D^0 \to X\mu^+\nu_\mu) = (7.86 \pm 1.15)\%\,.$$

In 1995, almost simultaneously, the ARGUS [82] and CLEO [83] collaborations measured the branching fraction of the decay $D^0 \to Xe^+\nu_e$. The method used by both groups was the one first developed by the HRS collaboration [84]. It is based on the fact that the energy release in the decay $D^{*+} \to \pi^+D^0$ amounts only to several MeV and, therefore, the slow charged pion produced in the decay process flies in practically the same direction as that of D^{*+}. The direction in which D^{*+} travels is close to the thrust axis of the event. (The thrust axis is the direction in which the sum of the squares of the projections of particle momenta is at its maximum.) Thus, by studying the distribution in the angle between the event thrust axis and the direction of motion of the slow pion from D^{*+} one can determine the number of events involving the c quark (or the related number of events involving the $\bar{c}$ quark). Figure 10 depicts the distributions in $\cos\Theta$, where Θ is the angle between the thrust axis and the pion's momentum, obtained by the ARGUS collaboration [82]. The peak in

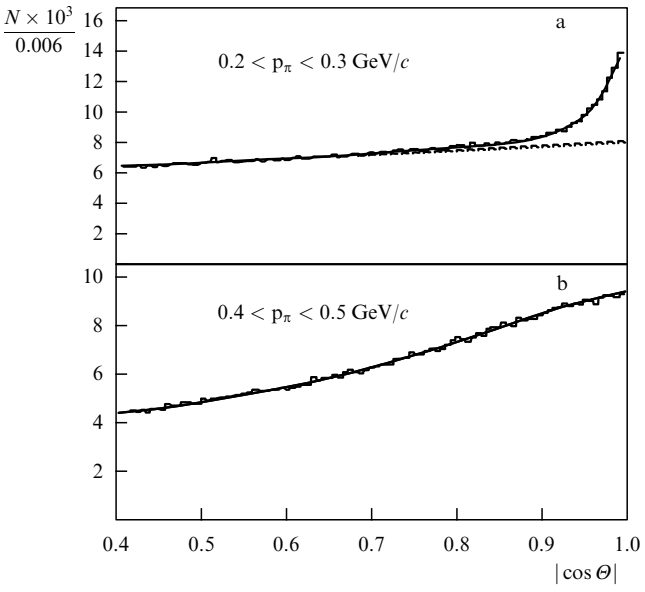

Figure 10. Distribution in $\cos\Theta$ for two ranges of pion momenta: (a) 0.2–0.3 GeV/c, and (b) 0.4–0.5 GeV/c.

Fig. 10a at $\cos\Theta \sim 1$ is a reflection of the contribution from the decay $D^{*+} \to \pi^+ D^0$, for which, at the energies used in the experiment, the greater number of pions have a momentum below 300 MeV/c. This conclusion is corroborated by the smoothness of the distribution in Fig. 10b, since the decay $D^{*+} \to \pi^+ D^0$ contributes nothing in the kinematic 400-to-500-MeV/c range. The number of $D^0 \to Xe^+\nu_e$ decays was determined by counting the number of events containing a slow pion moving at a small angle to the thrust axis and a positron. When this procedure was employed, the number of selected events involving the c quark proved to be several times larger than in the case of complete reconstruction of charmed hadrons. The values of $Br(D^0 \to Xe^+\nu_e)$ obtained by the ARGUS and CLEO collaborations are $(6.9 \pm 0.3 \pm 0.5)\%$ [82] and $(6.97 \pm 0.18 \pm 0.30)\%$ [83], respectively.

The ARGUS group also measured the branching fraction of the decay $D^0 \to X\mu^+\nu_\mu$ [82] and found that

$$Br(D^0 \to X\mu^+\nu_\mu) = (6.0 \pm 0.7 \pm 1.2)\% .$$

Averaging over the results of all measurements yields

$$Br(D^+ \to Xl^+\nu) = (17.2 \pm 1.9)\% ,$$

$$Br(D^0 \to Xl^+\nu) = (7.14 \pm 0.32)\% .$$

By using the values of the lifetimes of the D^0 and D^+ mesons listed in Table 8 one can obtain the following expressions for the widths of the semileptonic decays of D^+ and D^0:

$$\Gamma(D^+ \to Xl^+\nu) = (16.3 \pm 1.8) \times 10^{10}\ s^{-1} ,$$

$$\Gamma(D^0 \to Xl^+\nu) = (17.2 \pm 0.8) \times 10^{10}\ s^{-1} .$$

Clearly, the widths of the semileptonic decays of D^+ and D^0 coincide to within errors, and their average value is

$$\Gamma(D \to Xl^+\nu) = (17.1 \pm 0.7) \times 10^{10}\ s^{-1} .$$

The fact that the widths of the semileptonic decays of D^0 and D^+ coincide suggests that the difference in the lifetimes of the D mesons is determined solely by the difference in the widths of the hadronic decays.

The keen attention of theoreticians to exclusive semileptonic decays of charmed particles can be explained by the fact that the characteristics of these decays can be determined more precisely by theoretical tools. Only the spectator diagram contributes to such processes and, which is no less important, estimating the decay probabilities does not involve uncertainties that emerge because of the interaction of the decay products of charmed particles.

Experimental studies of semileptonic decays are hindered by the presence (in addition to charged particles) of neutrinos in such decays ($D \to Kl\nu$, $D \to K^*l\nu$, $D_s \to \phi l\nu$). In view of this, the D mesons that decay in a semileptonic manner cannot be reconstructed completely from the decay products, so that to determine the branching fraction of such decays one must study the distributions in the invariant mass of Kl, K^*l, or ϕl.

The main sources of the background in studies of semileptonic decays in experiments involving electron–positron colliders are as follows:

(1) the combination of a real kaon and a hadron misidentified as a lepton;

(2) a real lepton that is the product of the semileptonic decay of a charmed particle and a kaon (ϕ) produced not by the decay of a charmed hadron but, for example, by fragmentation of light quarks;

(3) a random combination Kl (ϕl), where the kaon and lepton are formed as a result of decays of B and $\bar{B}$ mesons, since to increase the statistics data are also used that are obtained at energies of the colliding beams equal to the mass of the $\Upsilon(4S)$ resonance, which decays to a $B\bar{B}$ pair.

An additional requirement that must be met in experiments involving a fixed target if we want to extract D mesons is that the products of the decay of the D meson must be ejected by a vertex that differs from the primary vertex. Such a requirement makes it possible to strongly suppress the contribution of the background source (2). Naturally, the background source (3) is also absent in fixed-target experiments. One should not forget, however, that charmed hadrons are produced in such experiments a hundred times more rarely, with the result that the contribution of the background source (1) is large in these experiments.

Until recently, there existed a strong discrepancy between theory and experiment in the estimate of the ratio of the probabilities of semileptonic decays of D mesons with the production of the pseudoscalar (K) and vector (K^*) mesons. The value of this ratio averaged over all the experimental data is

$$\frac{Br(D \to \bar{K}^*l^+\nu)}{Br(D \to Kl^+\nu)} = 0.56 \pm 0.05\ [34] .$$

At the same time, in the simplest theoretical approaches this ratio does differ too much from unity, and even with allowance for possible corrections the theoreticians for a long time predicted the value of this ratio as being between 0.8 and 1.2 [85].

Only lately appeared theoretical papers [86–88] capable of reproducing the experimentally observed values of this ratio. Let us discuss this problem in greater detail. The diagram of such a decay is shown in Fig. 5a. The differential

form of the width of the decay $D \to Kl\nu$ can be written

$$\frac{d\Gamma}{dq^2} = \frac{G_F^2}{24\pi^3} |V_{cs}|^2 P_K^3 f_+(q^2) .$$

The weak interaction is represented in the amplitude by the product $G_F V_{cs}$, where V_{cs} is the matrix element of the transition from the c quark to the s quark. If the lepton mass is ignored, the effect of the strong interaction is fully described by the form-factor $f_+(q^2)$ alone. This form-factor specifies the amplitude of the process of formation of the K meson from the pair $(s\bar{q})$, with $q^2 = M^2(l\nu)$ the square of the momentum transferred by the c quark.

In the case of the decay $D \to K^*$ we have three form-factors: $A_1(q^2)$, $V(q^2)$, and $A_2(q^2)$. In this case the expression for the amplitude of the semileptonic decay is much more complicated [68]. The form-factor A_1 contributes the most. The form-factor ratio is determined by fitting the corresponding angular distributions among the secondary particles. When doing the fitting, it is also assumed that the q^2-dependence of these form-factors is the same as in the form-factor for the decay $D \to K$. So far only two form-factors have been measured fairly accurately: $f_+(q^2)$ and $A_1(q^2)$. Their values at $q^2 = 0$ are $f_+(0) = 0.76 \pm 0.03$ and $A_1(0) = 0.56 \pm 0.04$. Almost all models yield an accurate value of the form-factor f_+ for the decay of the D meson with the formation of the pseudoscalar K meson. At the same time, quark models [85] yield an overestimated value of A_1, which overvalues the probability of the decay $D \to K^*$ by a factor of two. Better agreement is achieved in models that use lattice calculations [88] and sum rules [86]. The other two form-factors for the decay to the vector meson $[A_2(0) = 0.39 \pm 0.08$ and $V(0) = 1.1 \pm 0.2]$ have not as yet been measured accurately enough to influence the choice of model.

The CLEO group [89] has also measured the semileptonic decays of D_s:

$$\frac{\mathrm{Br}(D_s^+ \to \phi e^+ \nu)}{\mathrm{Br}\left(D_s^+ \to (\eta + \eta')e^+\nu\right)} = 0.60 \pm 0.06 \pm 0.06 ,$$

where the statistical and systematic errors of measurement are presented separately. Clearly, this value is in good agreement with the value of the similar ratio of D mesons.

7.2 Cabibbo-suppressed semileptonic decays of charmed mesons

At present the volume of statistics collected makes it possible to study such rare processes as CS semileptonic decays ($D \to \pi l\nu$, $D \to \rho l\nu$). The ratio of the CS and CA semileptonic decays of D mesons with the formation of a pseudoscalar meson can be used to determine the product of the matrix-element ratio and the form-factor ratio. In particular,

$$\frac{\mathrm{Br}(D^0 \to \pi^- e^+ \nu_e)}{\mathrm{Br}(D^0 \to K^- e^+ \nu_e)} = 2\,\frac{\mathrm{Br}(D^+ \to \pi^0 e^+ \nu_e)}{\mathrm{Br}(D^+ \to \bar{K}^0 e^+ \nu_e)} = 1.97 \left|\frac{V_{cd}}{V_{cs}}\right|^2 \left[\frac{f_+^\pi(0)}{f_+^K(0)}\right]^2 .$$

The measured value of the branching fraction of the decay $D^0 \to \pi^- l^+ \nu$ can be used to improve the value of the matrix element V_{ub}. The form-factor of the CS decay $b \to u$ can be expressed in terms of a similar form-factor for the transition $c \to d$ with the same 4-momentum transfer [90]. Since knowing the form-factor for the semileptonic decay $b \to u$ is necessary if we want to find V_{ub} in a model-independent way, the study of semileptonic decays $c \to d$ will lead to a more accurate value of V_{ub}.

The CLEO [91] and E687 [92] groups measured the branching fraction of the CS semileptonic decay $D^0 \to \pi^- e^+ \nu$ and found, respectively, 87 ± 33 and 91 ± 18 such events. In both cases the decay $D^{*+} \to D^0 \pi^+$ was used to separate the processes being investigated. These results can be compared with the results of the MARK III collaboration, where 7 decays $D^0 \to \pi^- e^+ \nu_e$ and 56 decays $D^0 \to K^- e^+ \nu_e$ were detected [93]. Using the decay $D^{*+} \to D^+ \pi^0$, the CLEO group reconstructed 100 ± 35 CS decay events, $D^+ \to \pi^0 e^+ \nu$ [94]. The values of the ratios of the branching fractions of semileptonic CS and CA decays are listed in Table 11. Using the existing value for the

Table 11. Ratios of branching fractions for the semileptonic Cabibbo-suppressed and Cabibbo-allowed decays of D mesons.

Experiment	Measured ratio	Measured value	Number of events
MARK III [93]	$\frac{\mathrm{Br}(D^0 \to \pi^- e^+ \nu_e)}{\mathrm{Br}(D^0 \to K^- e^+ \nu_e)}$	$0.057^{+0.038}_{-0.017} \pm 0.005$	7
CLEO II [91]	$\frac{\mathrm{Br}(D^0 \to \pi^- l^+ \nu)}{\mathrm{Br}(D^0 \to K^- l^+ \nu)}$	$0.103 \pm 0.039 \pm 0.013$	87 ± 33
E687 [92]	$\frac{\mathrm{Br}(D^0 \to \pi^- l^+ \nu)}{\mathrm{Br}(D^0 \to K^- l^+ \nu)}$	$0.101 \pm 0.020 \pm 0.003$	91.0 ± 17.8
CLEO II [94]	$\frac{\mathrm{Br}(D^+ \to \pi^0 l^+ \nu)}{\mathrm{Br}(D^+ \to \bar{K}^0 l^+ \nu)}$	$0.046 \pm 0.014 \pm 0.017$	100 ± 35
E653 [95]	$\frac{\mathrm{Br}(D^+ \to \rho^0 \mu^+ \nu_\mu)}{\mathrm{Br}(D^+ \to \bar{K}^{*0} \mu^+ \nu_\mu)}$	$0.044^{+0.031}_{-0.025} \pm 0.014$	$4.0^{+2.8}_{-2.3}$
E687 [96]	$\frac{\mathrm{Br}(D^+ \to \rho^0 \mu^+ \nu_\mu)}{\mathrm{Br}(D^+ \to \bar{K}^{*0} \mu^+ \nu_\mu)}$	$0.079 \pm 0.019 \pm 0.013$	32.9 ± 9.0
E791 [97]	$\frac{\mathrm{Br}(D^+ \to \rho^0 l^+ \nu)}{\mathrm{Br}(D^+ \to \bar{K}^{*0} l^+ \nu)}$	0.047 ± 0.013	103 ± 25

matrix-element ratio,

$$\left|\frac{V_{cd}}{V_{cs}}\right|^2 = 0.051 \pm 0.002\,,$$

we arrive at the following value for the ratio of the decay constants:

$$\frac{f_+^{\pi}(0)^2}{f_+^{K}(0)} = 1.2 \pm 0.3\,.$$

This result agrees with the predictions of a broad spectrum of models, with the value ranging from 0.7 to 1.4.

Table 11 also lists all the existing experimental data on the ratio

$$\frac{\mathrm{Br}(D^+ \to \rho^0 l^+ \nu_l)}{\mathrm{Br}(D^+ \to \bar{K}^{*0} l^+ \nu)}\,.$$

The E653 collaboration was the first to detect $4.0^{+2.8}_{-2.3}$ events of the decay $D^0 \to \rho^0 \mu^+ \nu_\mu$ [95]. Soon after the E687 [96] and E791 [97] collaborations detected this decay with a much larger volume of statistics. The value of $\mathrm{Br}(D^+ \to \rho^0 l^+ \nu_l)/\mathrm{Br}(D^+ \to \bar{K}^{*0} l^+ \nu)$ is sensitive mainly to the form-factor A_1. The experimental value proves to be much larger than the value predicted by various quark models and can be explained only by the latest QCD calculations on lattices [88] and in several other models [98].

Finally, the CLEO group [94] found an upper limit on the branching fraction of the semileptonic decay $D^+ \to \eta l^+ \nu$:

$$\frac{\mathrm{Br}(D^+ \to \eta l^+ \nu)}{\mathrm{Br}(D^+ \to \pi^0 l^+ \nu)} < 1.5\,.$$

Table 12 lists the data on the exclusive modes of semileptonic decays of D mesons and the upper limits on the probabilities of other semileptonic decays. Clearly, so far only semileptonic decays of charmed mesons with the production of a pseudoscalar particle (K, π) or a vector particle (K^*, ρ) have been detected. At the same time, only weak upper limits have been established for the decays of D mesons with the formation of excited states of K mesons. Nevertheless, it is possible that the detected CA and CS decays to the pseudoscalar and vector mesons saturate the inclusive width of the semileptonic decay, although the existing discrepancy between the value of the inclusive width of the semileptonic decay and the sum of the widths of the detected exclusive decays exceeds three standard deviations.

Table 12. Widths of semileptonic decays of D mesons.

Decay channel	Source	Decay width, 10^{10} s^{-1}
$D \to \bar{K} l^+ \nu$	PDG [34]	8.2 ± 0.5
$D \to K^* l^+ \nu$	PDG [34]	4.4 ± 0.4
$D \to \pi l^+ \nu$	[91–94]	0.8 ± 0.2
$D \to (\rho, \omega, \eta, \eta') l^+ \nu$	[87]	~ 0.4
Total for exclusive channels		13.8 ± 0.7
Inclusive channel	PDG [34]	17.1 ± 0.7
$D^+ \to (K^-\pi^+)_{NR} e^+ \nu_e$	E691 [103]	< 0.7
$D^+ \to (K^-\pi^+)_{NR} \mu^+ \nu_\mu$	E687 [104]	< 0.4
$D^+ \to (K\pi)_{NR} \pi e \nu_e$	E691 [105]	< 0.9
$D^+ \to \bar{K}^{*0} \pi e^+ \nu_e$	E691 [103]	< 1.1
$D^+ \to \bar{K}^{*0} \pi^0 \mu^+ \nu_\mu$	E687 [104]	< 0.2
$D^0 \to K^-\pi^+\pi^-\mu^+\nu_\mu$	E653 [106]	< 0.3
$D^0 \to (K^*\pi)^-\mu^+\nu_\mu$	E653 [106]	< 0.4

7.3 Semileptonic decays of charmed baryons

The results of predictions for semileptonic decays of baryons strongly depend on the model of the wave function of the heavy baryon and the nature of the q^2-dependence of the hadronic form-factor. The experimental data on semileptonic decays of baryons provide the information necessary if we want to select the best theoretical model.

The ARGUS [99] and CLEO [100] collaborations contributed the most to the detection of semileptonic decays of charmed baryons. Table 13 lists the results of these experiments in measuring the probabilities of semileptonic decays. The decay $\Lambda_c^+ \to \Lambda l^+ \nu$ was also studied in other experiments. The MARK II group [101] measured $\mathrm{Br}(\Lambda_c^+ \to e^+ X) = (4.7 \pm 1.5)\%$ and $\mathrm{Br}(\Lambda_c^+ \to \Lambda e^+ X) = (1.1 \pm 0.8)\%$. A 15-foot chamber placed in the neutrino beam at Fermilab was used to establish the upper limit $\mathrm{Br}(\Lambda_c^+ \to \Lambda e^+ X) < 2.2\%$ at a 90% confidence level [102].

Table 13. Probabilities of semileptonic decays of baryons in picobarns.

Decay channel	ARGUS	CLEO II
$\sigma(e^+e^- \to \Lambda_c^+ X)\,\mathrm{Br}(\Lambda_c^+ \to \Lambda e^+ X)$	$4.20 \pm 1.28 \pm 0.71$	$4.87 \pm 0.28 \pm 0.69$
$\sigma(e^+e^- \to \Lambda_c^+ X)\,\mathrm{Br}(\Lambda_c^+ \to \Lambda \mu^+ X)$	$3.91 \pm 2.02 \pm 0.90$	$4.43 \pm 0.51 \pm 0.64$
Mean value	$4.15 \pm 1.03 \pm 1.18$	$4.77 \pm 0.25 \pm 0.66$
$\sigma(e^+e^- \to \Xi_c^0 X)\,\mathrm{Br}(\Xi_c^0 \to \Xi^- e^+ X)$		$0.63 \pm 0.12 \pm 0.10$
$\sigma(e^+e^- \to \Xi_c^0 X)\,\mathrm{Br}(\Xi_c^0 \to \Xi^- l^+ X)$	$0.74 \pm 0.24 \pm 0.09$	
$\sigma(e^+e^- \to \Xi_c^+ X)\,\mathrm{Br}(\Xi_c^+ \to \Xi^0 e^+ X)$		$1.55 \pm 0.33 \pm 0.25$

Using the averaged result of the ARGUS and CLEO collaborations for the semileptonic decay of Λ_c^+ from Table 13 and the result of the same collaborations for

$$\sigma(e^+e^- \to \Lambda_c^+ X)\mathrm{Br}(\Lambda_c^+ \to pK^-\pi^+) = (11.3 \pm 0.8 \pm 1.0)\ \mathrm{pb},$$
$$\mathrm{Br}(\Lambda_c^+ \to pK^-\pi^+) = (4.3 \pm 1.1)\%$$

we can find the branching fraction of the semileptonic decay of Λ_c^+:

$$\mathrm{Br}(\Lambda_c^+ \to \Lambda l^+ X) = (1.7 \pm 0.4)\%\,.$$

Multiplying this value by the lifetime of Λ_c, i.e. by $\tau_{\Lambda_c^+} = (2.00 \pm 0.11) \times 10^{-13}$ s yields the value of the width of the semileptonic decay:

$$\Gamma(\Lambda_c^+ \to \Lambda l^+ X) = (8.5 \pm 2.1) \times 10^{10}\ \mathrm{s}^{-1}\,,$$

which is much smaller than the width of the semileptonic decay of the D meson,

$$\Gamma(D \to X l^+ \nu) = (17.1 \pm 0.7) \times 10^{10}\ \mathrm{s}^{-1}\,.$$

At the same time, the simplest spectator model predicts that the widths of the semileptonic decays of charmed baryons and mesons are equal. To resolve this contradiction and to be able to compare in greater detail the branching fractions of semileptonic decays of charmed baryons with theoretical models, the accuracy of the experimental results must be increased significantly. There is every reason to believe this will soon be done.

8. Nonleptonic decays of charmed hadrons

The number of discovered decay channels for D mesons already amounts to several hundred [34]. Naturally, even a brief description of such a number of decay channels is impossible, whereby in this review we will discuss only some of the most interesting cases (from the viewpoint of the author).

8.1 Measurements of the absolute branching fractions for D-meson decays

To determine the branching fraction of any D-meson decay channel we must know the number of D mesons produced and the number of such D mesons that have decayed via the channel in question. By dividing the second number by the first we arrive at the branching fraction of the decay under investigation. Until recently one had to rely, in determining the number of D mesons produced, on theoretical estimates, whose accuracy was no higher than 10–20%. At the same time, the volume of statistics gathered in experiments makes it possible to achieve an accuracy of about 1%. To avoid making theoretical estimates, it is enough to determine, through experiments, the absolute branching fraction for at least one decay channel for D^0, D^+, and D_s^+, respectively, and then use this channel as the normalization channel. The branching fraction of a D-meson decay via any channel is equal to the ratio of the number of decays registered in the specified channel to the number of decays registered in the normalization channel multiplied by the branching fraction via the normalization channel.

Such a method of calculating the branching fraction of decay via any channel introduces an error in measuring the normalization channel, so that the probability of decay via the normalization channel must be found as accurately as possible. Hence the normalization channels are selected from the decay channels that can easily be measured, i.e. channels with a high decay probability and only charged particles in the final state. For D^0, D^+, and D_s^+ such channels are $D^0 \to K^-\pi^+$, $D^+ \to K^-\pi^+\pi^-$, and $D_s^+ \to \phi\pi^+$, respectively. The idea of determining the branching fraction for normalization channels is based on the fact that, in the interactions that take place in electron–positron colliders, the production of a c quark is always accompanied by the production of a $\bar{c}$ quark. Hence, if we select events with a $\bar{c}$ quark and count the cases in which, on the other hand, the D meson containing a c quark decays via the channel of interest to us, we can determine the absolute branching fraction of the normalization channel. Undoubtedly, the easiest way to do all this is to completely reconstruct all the mesons with the $\bar{c}$ quark, and, in the events where this was achieved, to reconstruct the D meson containing the c quark in the channel in question. Employing these techniques, the MARK III collaboration [107] was able to measure the absolute branching fraction of the decay $D^0 \to K^-\pi^+$. Unfortunately, the need to reconstruct two charmed hadrons markedly reduces the statistical accuracy of the measurements.

However, recently a method has been developed that significantly increases the accuracy of the measurements. The method was first used by the HRS collaboration [84] (see Section 7.1). The number of D^0 mesons was found by counting the number of slow pions produced in the decay $D^{*+} \to \pi^+ D^0$ and ejected at small angles to the thrust axis of an event, while the reconstruction in these events of D^0 mesons in the decay channel $D^0 \to K^-\pi^+$ was used to determine the branching fraction. Using the method of Abachi et al. [84], the researchers succeeded in increasing the accuracy of measuring the absolute branching fraction of the decay $D^0 \to K^-\pi^+$ from 13% in the MARK III experiment to 4% for the sum of the ALEPH, CLEO, and ARGUS measurements [108].

The CLEO group used a similar method to measure the absolute branching fraction of the decay $D^+ \to K^-\pi^+\pi^+$. In this case the number of D^+ mesons was determined by using the distribution in the angle of ejection of the slow π^0 in the decay $D^{*+} \to \pi^0 D^+$. Using an excellent electromagnetic calorimeter consisting of CsI crystals, which made it possible to determine exactly the direction of motion of a neutral pion produced in the decay of D^{*+}, the CLEO collaboration significantly increased the accuracy of measuring the absolute branching fraction of the decay $D^+ \to K^-\pi^+\pi^+$ [109].

Finally, in the mid-1990s, the BES [110] and CLEO [111] collaborations measured the absolute branching fraction of the decay $D_s^+ \to \phi\pi^+$. All previous measurements used theoretical models or estimates for determining the number of produced D_s^+. For instance, the formula used to determine the probability of this decay was [68]

$$\mathrm{Br}(D_s^+ \to \phi\pi^+) = F\,\mathrm{Br}(D^+ \to \bar{K}^{*0}e^+\nu)\,\frac{\Gamma(D_s^+ \to \phi\pi^+)}{\Gamma(D_s^+ \to \phi e^+\nu)}\,\frac{\tau(D_s^+)}{\tau(D^+)}\,,$$

where F stands for the theoretical predictions for

$$\frac{\Gamma(D_s^+ \to \phi e^+\nu)}{\Gamma(D^+ \to \bar{K}^{*0}e^+\nu)}\,.$$

To determine the probability of the decay $D_s^+ \to \phi\pi^+$, the BES collaboration used the events $e^+e^- \to D_s^+ D_s^-$, in which one or both D_s mesons were completely reconstructed. Unfortunately, the result of this research was based solely on two events, which makes for moderate accuracy.

The CLEO collaboration did a model-independent measurement of the probability ratio

$$\frac{\mathrm{Br}(D_s^+ \to \phi\pi^+)}{\mathrm{Br}(D^0 \to K^-\pi^+)} = 0.92 \pm 0.20 \pm 0.11\,,$$

by employing the method of partial reconstruction of the decay $\bar{B}^0 \to D^{*+} D_s^{*-}$ [111].

The averaged absolute values of the decay probabilities for normalization channels are listed in Table 14.

Table 14. Absolute branching fractions averaged over all the experiments.

Decay channel	Branching fraction, %
$D^0 \to K^-\pi^+$	3.86 ± 0.14
$D^+ \to K^-\pi^+\pi^+$	9.1 ± 0.7
$D_s^+ \to \phi\pi^+$	3.6 ± 0.9

8.2 Contribution of the W-exchange diagram to decays of charmed hadrons

As noted earlier, the contribution of the W-exchange diagram to the decays of D mesons is suppressed due to the violation of the helicity conservation law (see Section 3). However, models exist in which, outside the scope of the SM, mechanisms are

suggested that weaken this suppression and which predict a high branching fraction of such decays (about 1%) [112]. To verify such models it was necessary to measure the branching fraction of the decay $D^0 \to \phi\bar{K}^0$. The contribution of the spectator diagrams to this decay is negligible, and the principal diagram is the W-exchange diagram (Fig. 5f). In 1985, the ARGUS collaboration announced the first measurement of the branching fraction of the given decay [113]. The measurement was repeated in 1987 [114] with a large volume of statistics, and the result was

$$\mathrm{Br}(D^0 \to \phi\bar{K}^0) = (0.82 \pm 0.17 \pm 0.08)\% .$$

Later this result was corroborated by other experiments. This unexpectedly high branching led to a large number of theoretical interpretations of the given result [115]. Still, at present it is assumed that the high branching fraction of the given decay is determined by interactions in the final state. Since the mass of a D^0 meson lies in the region with many resonances, the effect of rescattering of the mesons produced by the decay of the D^0 meson increases substantially. Such rescattering can lead to a situation in which the ϕ and K are not the decay products of D^0 but are formed in the process of rescattering of the true decay products of D^0. Figure 11 depicts a decay process in which the spectator diagram provides the principal contribution. A possible result of this decay is the emergence of ϕ and K mesons in the final state [116].

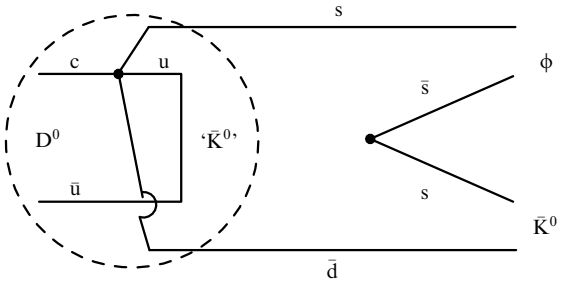

Figure 11. Decay of a c quark followed by the annihilation of quarks and the interaction in the final state for $D^0 \to \bar{K}^0\phi$. The region inside the dashed circle describes the subprocess $D^0 \to$'$\bar{K}^0$', where the '$\bar{K}^0$'-state 'carries' the quantum numbers of the $\bar{K}^0$ meson.

8.3 Cabibbo-suppressed decays of charmed hadrons

Studies of CS decays of D mesons (Fig. 5g, h) have contributed substantially to the understanding of decays of charmed hadrons and helped in developing theoretical models. In view of the fact that the probability of CS decays is 20 times lower than the probability of CA decays, Cabibbo-suppressed decays have been intensively studied only in the last decade, i.e. after the experiments reached the necessary level of statistical accuracy. It is in the CS decays that one can study the interrelationship of the interaction, responsible for the decay, and the strong interaction, which manifests itself in the final state.

An interesting problem that has attracted much attention in the last decade is that of finding the ratio of the probabilities of $D^0 \to K^-K^+$ and $D^0 \to \pi^-\pi^+$. If we remain within the SU(3)-symmetry setting, the expected value for this ratio is close to unity [117]. However, the first values measured by the MARK II [118] and MARK III [119] collaborations proved to be close to 3.5, although the errors were large. At present, the value averaged over all the results of experimental measurements is [34]

$$\frac{\Gamma(D^0 \to K^+K^-)}{\Gamma(D^0 \to \pi^+\pi^-)} = 2.86 \pm 0.28 .$$

There are many theoretical approaches [120] used to explain this experimental value. What is most important here are the interactions in the final state. Attempts have been made to explain the fact that the experimental value exceeds the theoretical by taking penguin diagrams into account and by using approaches based on QCD rules and unperturbed algebraic approximations. Measurements of this ratio with high accuracy will make it possible to check the validity of the different theoretical models and will help in refining the contribution of long-distance effects in $D^0\bar{D}^0$ mixing [121].

9. $D^0\bar{D}^0$-mixing and CP-symmetry violation effects in D-meson decays

9.1 $D^0\bar{D}^0$ mixing

In the SM, the $D^0 \to \bar{D}^0$ transition is represented by the diagram depicted in Fig. 12, but its probability is strongly suppressed in comparison to the probabilities of similar transitions $K^0 \to \bar{K}^0$ and $B^0 \to \bar{B}^0$. Nevertheless, studies of $D^0\bar{D}^0$ mixing not only make it possible to extract additional information about transformations of this kind but are also extremely interesting from the standpoint of developing new approaches that differ from the SM. It is the weakness of the mixing effects in the SM that will help in identifying a new approach.

Generally, the value of $D^0\bar{D}^0$ mixing, r_{mix}, is specified by fixing two dimensionless parameters, $x_D = \delta m/\gamma_+$ and $y_D = \gamma_-/\gamma_+$, where $\gamma_\pm$ and δm are defined as $\gamma_\pm = (\gamma_1 \pm \gamma_2)/2$ and $\delta m = m_2 - m_1$, with m_i and γ_i $(i = 1, 2)$ the masses and widths of decay of two CP eigenvalues (-1 and $+1$). Assuming that the mixing is weak (as in the case for D mesons), i.e. $\delta m, \gamma_- \ll \gamma_+$ (and, hence, $x_D, y_D \ll 1$), we find that $r_{\mathrm{mix}} = (x_D^2 + y_D^2)/2$. Mixing exists if either x_D is not zero (i.e. due to the $D^0 - \bar{D}^0$ transitions) or y_D is not zero (i.e. due to the fact that the fast component decays while the slow component, which is a mixture of D^0 and $\bar{D}^0$, remains). Theoretical estimates of the probability of $D^0\bar{D}^0$ mixing contain a large uncertainty. While the contribution of short-distance effects of the diagram in Fig. 12 is known to a high accuracy [122] and is of order 10^{-10}, the contribution of long-distance effects may vary from 10^{-7} to 10^{-4} [123].

Interest in $D^0\bar{D}^0$ mixing grew considerably after the publication in 1985 of the results of the MARK III

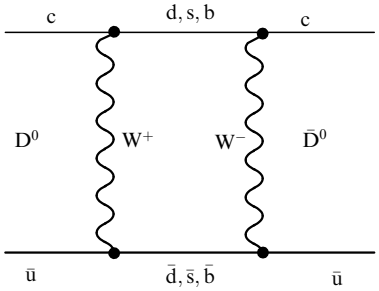

Figure 12. Box diagram.

collaboration [124]. The group reported the discovery of three events in one of which the charmed mesons were reconstructed from the final states, $K^+\pi^-$ and $K^+\pi^-\pi^0$, while in the other events the charmed mesons decayed to the final states $K^+\pi^-\pi^0$ and $K^+\pi^-\pi^0$. The existence of such events can be explained either by the existence of $D^0\bar{D}^0$ mixing or by the fact that D^0 or $\bar{D}^0$ decayed via a DCS channel. For the two limits, i.e. decay only via DCS channels or via mixing, Gladding et al. [124] arrived at the following limitations:

(1) if the given result is determined solely by mixing in the absence of a contribution from DCS decay, $r_{\rm mix} = 0.012 \pm 0.006$ or $r_{\rm mix} > 0.004$ at 90% confidence level; and

(2) if the given result is determined solely by DCS decay in the absence of a contribution from $D^0\bar{D}^0$ mixing, the DCS decay to CA decay probability ratio $r_{\rm DCS} = (7 \pm 4)\tan^4\theta_{\rm C}$ or $r_{\rm DCS} > 1.9\tan^4\theta_{\rm C}$ at 90% confidence level.

The search for $D^0\bar{D}^0$ mixing in experiments is possible in both hadronic decays and in semileptonic decays of D mesons.

9.2 Search for $D^0\bar{D}^0$ mixing in hadronic decays

The method is based on the search for the decay $D^0 \to K^+\pi^-(X)$. Such a final state in the decay of the D^0 meson may emerge either as a result of the $D^0 \to \bar{D}^0$ transition followed by the CA decay $\bar{D}^0 \to K^+\pi^-(X)$ or as a result of the DCS decay $D^0 \to K^+\pi^-(X)$. The main difficulty in this method lies in the fact that the contribution of $D^0\bar{D}^0$ mixing is a hundred times weaker than the contribution of the DCS decay. The ratio

$$r_{\rm DCS}^{K\pi} = \frac{\Gamma(D^0 \to K^+\pi^-)}{\Gamma(D^0 \to K^-\pi^+)}$$

is predicted to be in the interval 0.0027 to 0.0054 [125].

There are at least two experimentally observable differences between $D^0\bar{D}^0$ mixing and DCS decays:

(1) the different time dependence of the decays of D^0 ($\bar{D}^0$) mesons; and

(2) the different resonance structure for DCS decays and for $D^0\bar{D}^0$ mixing in the decays $D^0 \to K^+\pi^-\pi^0, K^+\pi^-\pi^+\pi^-$.

The difference in the time dependence has been used in studies of the decay $D^0 \to K^+\pi^-$. The ratio of the widths of the decays $D^0 \to K^+\pi^-$ and $D^0 \to K^-\pi^+$ vary with time in the following manner:

$$r_{\rm D}^{K\pi}(t) = \frac{\Gamma(D^0(t) \to K^+\pi^-)}{\Gamma(D^0 \to K^-\pi^+)} \sim r_{\rm mix}^{K\pi}(t) + r_{\rm DCS}^{K\pi} + r_{\rm int}^{K\pi}(t)\,.$$

Here $r_{\rm mix}^{K\pi}$ and $r_{\rm DCS}^{K\pi}$ are the contributions of the $D^0\bar{D}^0$ mixing and DCS decays, respectively, and the interference term

$$r_{\rm int}^{K\pi}(t) = 2\sqrt{r_{\rm mix}^{K\pi}(t)}\,\sqrt{r_{\rm DCS}^{K\pi}}\,\cos\phi\,,$$

where ϕ is the unknown phase. In this expression, $r_{\rm DCS}^{K\pi}$ is time-independent, $r_{\rm int}^{K\pi}(t) \propto t$, and, finally, $r_{\rm mix}^{K\pi}(t) \propto t^2$. Thus, by studying the dependence of $r_{\rm D}^{K\pi}(t)$ on the decay time of D^0 one can separate the contributions the DCS decays from that of $D^0\bar{D}^0$ mixing.

To separate the rare DCS decay $D^0 \to K^+\pi^-$ from the CA decay $\bar{D}^0 \to K^+\pi^-$, investigations of D^0 from the decay $D^{*+} \to D^0\pi^+$ were made. Events were selected that contain a slow pion of the same sign as the kaon from the decay of D^0, and for such events the distribution in the mass difference $\Delta M = M(D^{*+}) - M(D^0) - M(\pi^+)$ was studied. Operating in this way, the E691 group [126] arrived at the following result: $r_{\rm mix} = 0.0005 \pm 0.002$, which corresponds to an upper limit on the mixing probability $r_{\rm mix} < 0.0037$. Note that this limit was obtained under an additional assumption that the interference term can be neglected. Although some theoreticians support this assumption, there is no common agreement on this aspect [127]. The E791 group [128] also studied the (incorrect in sign) combinations in the following decay chain: $D^{*+} \to \pi^+D^0$ followed by $D^0 \to K^+\pi^-$ or $D^0 \to K^+\pi^-\pi^+\pi^-$. The researchers set the upper bound on the mixing probability at $r_{\rm mix} < 0.0085$ without making any assumptions about the magnitude of the interference term.

The decay $D^0 \to K^+\pi^-$ was first detected in the CLEO experiment [129]. The experimenters registered 19 ± 6 events, which corresponds to

$$\frac{\Gamma(D^0 \to K^+\pi^-)}{\Gamma(D^0 \to K^-\pi^+)} = 0.0077 \pm 0.0025 \pm 0.0025\,.$$

However, they were unable to measure the time dependence of this decay and, hence, to determine unequivocally the cause of this dependence.

The E791 experiment presented possibilities for temporal separation of the two effects, but unfortunately the volume of the statistics was insufficient. Even if one were to assume that the contribution of mixing is zero, for the decay $D^0 \to K^+\pi^-$ there is a 2σ excess above the background [128]:

$$\frac{\Gamma(D^0 \to K^+\pi^-)}{\Gamma(D^0 \to K^-\pi^+)} = 0.0068^{+0.0034}_{-0.0033} \pm 0.0007\,.$$

For the decay $D^0 \to K^+\pi^-\pi^+\pi^-$ the value was

$$\frac{\Gamma(D^0 \to K^+\pi^-\pi^+\pi^-)}{\Gamma(D^0 \to K^-\pi^+\pi^-\pi^+)} = 0.0025^{+0.0036}_{-0.0034} \pm 0.0003\,.$$

The E687 group of experimenters [130] reconstructed 20.9 ± 6.6 events of the DCS decay $D^+ \to K^+\pi^-\pi^+$. The ratio of the branching fraction of this decay to that of the CA decay $D^+ \to K^-\pi^+\pi^+$ amounted to

$$\frac{\Gamma(D^+ \to K^+\pi^-\pi^+)}{\Gamma(D^+ \to K^-\pi^+\pi^+)} = 0.0072 \pm 0.0023 \pm 0.0017\,.$$

The E791 [131] reconstructed 59 ± 13 events. The ratio of the branching fraction of this decay to that of the CA decay $D^+ \to K^-\pi^+\pi^+$ amounted to

$$\frac{\Gamma(D^+ \to K^+\pi^-\pi^+)}{\Gamma(D^+ \to K^-\pi^+\pi^+)} = 0.0077 \pm 0.0017 \pm 0.0008\,.$$

There is every reason to believe that the resonance structure for DCS decays differs from that of the CA decay of D^0 that followed the $D^0 \to \bar{D}^0$ transition (for more details see, for instance, Ref. [132]).

9.3 Search for $D^0\bar{D}^0$ mixing in semileptonic decays

The method is based on studying the semileptonic decay $D^0 \to Kl\nu$, to which DCS decays do not contribute. Information about $D^0\bar{D}^0$ mixing in this case is extracted by comparing the number of events involving a correct-sign lepton (i.e. produced in the decay $D^0 \to K^-l^+\nu$) with the number of events involving an incorrect-sign lepton (i.e. produced in the

decay $\bar{D}^0 \to K^+ l^- \nu$). There is no need to analyze the time dependence, and it is sufficient to select the events in which D^0 and $\bar{D}^0$ decay in a semileptonic manner. Then, the normal decay of D^0 and $\bar{D}^0$ produces leptons of different signs, while $D^0\bar{D}^0$ mixing produces leptons of the same sign. This method was used in the E615 experiment [133], in which charmed particles were produced as a result of the interaction of 225-GeV pions and a fixed tungsten target. Counting the number of pairs of muons of the same sign, Louis et al. [133] found an upper bound on the mixing probability: $r_{\text{mix}} < 0.0056$ at 90% confidence level. Note that this result was obtained under the assumption that the production cross section for a charmed quark increases linearly with the atomic number of the nucleus of the target's material. A slower growth in the cross section will lead to a lower limit on the mixing probability.

9.4 Search for CP-symmetry violation in decays of D^0

CP-symmetry violation in the SM is determined by the complex-valued phase in the Kobayashi – Maskawa matrix [69], which describes the transition between quarks. So far CP-symmetry violation has been detected only in studies of neutral kaons. The SM predicts that CP asymmetry is large in decays of B mesons [134]. In the next few years several facilities, whose main goal will be to detect CP-symmetry violation in the decays of B mesons, will become operational [135]. In contrast to B mesons, the CP asymmetry is expected to be much weaker in the decays of charmed particles [136]. Hence the decays of charmed particles can be used to check the SM and to look for phenomena that lie outside the scope of the SM [137].

CP-symmetry violation leads to a difference in the branching fractions of decays of D^0 mesons to the final state f and to the complex-conjugate state $\bar{f}$. Such asymmetry requires the interference of at least two independent processes with a finite relative phase. There are three different types of possible CP-asymmetry signals in the decays of neutral D^0.

1. CP asymmetry in $D^0\bar{D}^0$ mixing. In this case the asymmetry emerges as a result of the interference of the direct decay of D^0 to the final state f and the process in which D^0 becomes $\bar{D}^0$ as a result of mixing with the subsequent decay $\bar{D}^0 \to f$. Within the SM, this asymmetry is expected to amount to 10^{-3}, but reliable estimates are hindered by the uncertainties inherent in the calculations of the contribution of long-distance effects.

2. CP asymmetry in direct decays. For such asymmetry to appear, the interactions in the final state must lead to a shift in the phase responsible for the strong interactions, with the phases responsible for the strong and weak interactions being different. In this case the asymmetry may emerge in the decays of neutral and charged mesons. The SM predicts that CP asymmetry in direct decays is the strongest in CS decays of D mesons ($\sim 10^{-3}$) [136].

3. Finally, CP asymmetry may emerge from the mutual influence of direct decay and $D^0\bar{D}^0$ mixing.

The search for CP asymmetry was carried out by the E691 [138], E687 [139], CLEO [140], and E791 [141] collaborations. The experimental accuracy of these measurements is close to 1%, and so far no CP-symmetry violation has been discovered at this level of accuracy.

9.5 Search for rare decays of D mesons

In recent years there has been a considerable increase in the upper limit on the branching fractions of particle decays that are rare and forbidden by the SM. Flavor-changing neutral currents (FCNC) incorporate the following processes: $D^0 \to l^+l^-$, $\gamma\gamma$ and $D \to X\gamma$, $X\nu\bar{\nu}$, Xl^+l^-, where l stands for an electron or muon. Such processes may occur via electromagnetic or weak penguin diagrams and sometimes due to the contribution of a diagram of the type depicted in Fig. 12. The contributions of short-distance effects are expected to be small [4] and can easily be calculated. Estimates of long-distance effects contain large uncertainties, so that it is more logical to speak of the upper limits on such contributions than of their specific values. Hewett's calculations [142] of the contribution of long-distance effects to the probability of the decay $D^0 \to \mu\mu$ lead to an upper limit of 3×10^{-15}, while for the $D^+ \to \pi^+ ee(\mu\mu)$ process the contribution does not exceed 10^{-8}. The detection of FCNC processes with probabilities exceeding those predicted by the SM will indicate that a new phenomena lying outside the scope of the SM has been discovered. The best upper limits on the branching fractions of such decays are given in Table 15, which also lists the upper limits on lepton number violating (LNV) decays and on lepton family number violating (LFNV) decays. (Note that these two types of decay are forbidden by the SM.) Such processes can easily be identified in experiments, and their presence will indicate that there are phenomena that cannot be described by the SM. However, at present all the experimental data in this area of physics are in good agreement with the SM predictions.

10. Prospects for charmed particle studies

In the near future there is sure to a breakthrough in the study of properties of charmed particles. Let us briefly discuss the experiments whose potential has not yet expired. These are necessarily the fixed-target experiments WA89 at CERN and E791 at Fermilab and the CLEO experiment at the electron – positron collider CESR.

At CERN, a WA89 detector was placed in a beam of 330-GeV Σ^--hyperons. The detector was used to measure the properties of baryons. Due to the fact that many more baryons are produced as a result of baryon – target interaction than as a result of the interaction of other particles and the target, the experimenters planned to detect and completely reconstruct from the decay products a record-breaking number of charmed baryons. The WA89 collaboration is still processing the data, and so far about 50% of the statistics gathered have been processed. There is every reason to believe that this research will produce new results on charmed baryons.

The E791 collaboration [28] hopes to increase the number of reconstructed charmed hadrons and exceed the statistics of the E687 collaboration by a factor of two. By using a beam of charged pions (in contrast to photons in the E687 experiment) the E791 experiment has an additional advantage, since the additional informational about the direction of motion of the particles impinging on the target can be used to reconstruct the charmed particles.

The CLEO III [149], a modification of the CLEO detector equipped with an extremely accurate vertex detector, will become operational very soon. The luminosity of the CESR accelerator will also be increased. Although the CLEO III detector is intended primarily for studies of B-meson properties, the huge number of charmed hadrons produced in the experiment gives rise to the hope that new results in the studies of properties of charmed particles will be obtained.

Table 15. Experimental upper limits on the rare and forbidden decays in the SM.

Type of decay	Decay channel	Best upper limit at 90% confidence level, $\times 10^{-5}$	Experiment
FCNC	$D^0 \to e^+e^-$	1.3	CLEO [143]
	$D^0 \to \mu^+\mu^-$	0.76	WA92 [144]
	$D^0 \to \rho^0 e^+e^- (\mu^+\mu^-)$	10 (23)	CLEO [143], E653 [145]
	$D^0 \to \pi^0 e^+e^- (\mu^+\mu^-)$	4.5 (18)	CLEO [143], E653 [145]
	$D^0 \to \eta e^+e^- (\mu^+\mu^-)$	11 (53)	CLEO [143]
	$D^0 \to \omega e^+e^- (\mu^+\mu^-)$	18 (83)	CLEO [143]
	$D^0 \to \phi e^+e^- (\mu^+\mu^-)$	5.2 (41)	CLEO [143]
	$D^0 \to \bar{K}^0 e^+e^- (\mu^+\mu^-)$	11 (26)	CLEO [143], E653 [145]
	$D^+ \to \pi^+ e^+e^- (\mu^+\mu^-)$	6.6 (1.8)	E791 [146]
	$D^+ \to K^+ e^+e^- (\mu^+\mu^-)$	20 (9.7)	E687 [147]
	$D^+ \to \rho^+\mu^+\mu^-$	58	E653 [145]
	$D_s^+ \to \pi^+\mu^+\mu^-$	43	E653 [145]
	$D_s^+ \to K^+\mu^+\mu^-$	59	E653 [145]
	$\Lambda_c \to p\mu^+\mu^-$	34	E653 [145]
LNV	$D^0 \to \mu^\pm e^\mp$	1.9	CLEO [143]
	$D^0 \to \pi^0\mu^\pm e^\mp$	8.6	CLEO [143]
	$D^0 \to \rho^0\mu^\pm e\mp$	4.9	CLEO [143]
	$D^0 \to \eta\mu^\pm e^\mp$	10	CLEO [143]
	$D^0 \to \omega\mu^\pm e^\mp$	12	CLEO [143]
	$D^0 \to \bar{K}^0\mu^\mp e^\pm$	10	CLEO [143]
	$D^+ \to \pi^+\mu^+e^-$	13	E687 [147]
	$D^+ \to \pi^+e^+\mu^-$	11	E687 [147]
	$D^+ \to \pi^+\mu^\pm e^\mp$	380	CLEO [148]
	$D^+ \to K^+\mu^+e^-$	12	E687 [147]
	$D^+ \to K^+e^+\mu^-$	13	E687 [147]
LFNV	$D^+ \to \pi^-e^+e^+$	11	E687 [147]
	$D^+ \to \pi^-\mu^+e^+$	11	E687 [147]
	$D^+ \to \pi^-\mu^+\mu^+$	8.7	E687 [147]
	$D^+ \to K^-e^+e^+$	12	E687 [147]
	$D^+ \to K^-\mu^+e^+$	13	E687 [147]
	$D^+ \to K^-\mu^+\mu^+$	12	E687 [147]
	$D^+ \to \rho^-\mu^+\mu^+$	56	E653 [145]
	$D_s^+ \to \pi^-\mu^+\mu^+$	43	E653 [145]
	$D_s^+ \to K^-\mu^+\mu^+$	59	E653 [145]
	$\Lambda_c^+ \to \Sigma^-\mu^+\mu^+$	70	E653 [145]

New fixed target experiments are becoming operational. These are primarily the E781 (SELEX) [150] and E831 (FOCUS) [151] detectors. While on older detectors the number of reconstructed charmed hadrons amounted to about 10^5, the goal of the new experiments is to reconstruct more than a million charmed hadrons. In 1996, the Fermilab started to gather data on the E781 detector, which uses a beam of hyperons. The goal is to detect hundreds of thousands of charmed baryons and, in particular, several thousands of Ω_c^0. The E831, a modification of the E687 detector that operated using a photon beam, will be used in the course of several years to detect and completely reconstruct a million charmed mesons and tens of thousands of charmed baryons. Note that in the new generation of experiments the background level will be reduced substantially by improving the method of particle identification and by increasing the accuracy of measurements.

There is also the COMPASS project [152]. The main objective of this experiment, with the respective detector becoming operational in the year 2000, is to study the spectroscopy of hadrons and, in particular, the spectroscopy of charmed hadrons. The detector will be placed in a 300-GeV pion beam of the SPS accelerator at CERN. The plan is to reconstruct several million charmed hadrons. An extended program to search of baryons consisting of two c quarks and one light quark will be implemented.

Another idea currently being developed is that of the CHARM-2000 detector [153]. The detector will become operational after the reconstruction of the main injector of the Tevatron (the proton – antiproton collider at Fermilab with a beam energy of about 1 TeV) is finished and the Tevatron's luminosity increases tenfold. The goal of the experiment is to reconstruct up to one hundred million charmed mesons, a million Λ_c^+, and tens of thousands of Ξ_c^+, Ξ_c^0, and Ω_c^0.

In the baryon sector, the increase of the statistics will lead to a better understanding of the properties of baryons. At the same time, in the case of charmed mesons the existing experimental detectors have yielded a statistical accuracy comparable to the value of systematic errors. Hence, in addition to the problem of increasing the volume of statistics, the primary goal is to dramatically improve the characteristics of the detector, which will make it possible to lower the level of systematic errors.

A project that has been actively discussed over the last ten years is that of building a special collider that would be used to study the physics of charmed hadrons and τ leptons and would therefore be called a tau-charm-factory [154]. Such a factory would be an electron–positron collider with a high luminosity ($L > 10^{33}$ cm^{-2} s^{-1}). It is assumed that the factory will operate in the range of 3 to 5.6 GeV in the center-of-mass system. This will make it possible, by gradually raising the energy, to study particles produced at practically threshold energies (i.e. at a beam energy equal to the sum of the rest masses of the particles in a pair) for the pairs $\tau^+\tau^-$, D^+D^-, $D^0\bar{D}^0$, $\Lambda_c^+\Lambda_c^-$, $\Sigma_c\bar{\Sigma}_c$, $\Xi_c\bar{\Xi}_c$, and $\Omega_c\bar{\Omega}_c$ (Table 16).

Table 16. Expected number of events during one year of operation of the tau-charm-factory at the listed energies and integral luminosities.

Type of event	Number of events per annum	Energy at center of mass, GeV	Integral luminosity, fb^{-1}
$D^0\bar{D}^0$	2.9×10^7	$\psi''(3.77)$	10
D^+D^-	2.1×10^7	$\psi''(3.77)$	10
$D_s^+D_s^-/D_s^\pm D_s^{*\pm}$	0.9×10^7	4.14	10
$\Lambda_c^+\Lambda_c^-$	0.3×10^7	4.8	3
$\Sigma_c\bar{\Sigma}_c$	0.1×10^7	5.2	2
$\Xi_c\bar{\Xi}_c$	0.3×10^6	5.2	2
$\Omega_c\bar{\Omega}_c$	0.3×10^5	5.6	1

The study of charmed particles at the production threshold has several advantages. First, the particle cross section is at its maximum, since it decreases in inverse proportion to the square of the energy at the center of mass. (Often, thanks to the presence of charmed resonances, e.g. $\psi''(3.77)$, which almost always decays to $D^0\bar{D}^0$ and D^+D^-, the production cross section for charmed particles proves to be much larger). Second, such studies take place in extremely favorable background conditions. Near their threshold the charmed particles are produced in the simplest final states, which contain only a charmed particle and antiparticle, with the result that there is not enough energy to produce additional hadrons. This ensures a high efficiency of selection, and the absence of additional particles and the simple normalization make it possible to determine the absolute values of the decay widths. Finally, near the threshold the charmed particles produced are almost at rest, with the result that the decay products of these hadrons have small momenta. Particles with such momenta are more easily identified.

The increase in the volume of the statistics of charmed hadrons by a factor of tens to hundreds will, unquestionably, lead to new interesting results and will make it possible to solve many problems. Below we list some of these problems:

1. Detailed (with a percent accuracy) measurements of the lifetimes of all charmed baryons stimulate theoretical progress in the quantitative description of relations between the lifetimes of charmed quarks.

2. Highly accurate measurements of the branching fractions of purely leptonic decays of mesons allows measuring the decay constants of charmed mesons with a good accuracy.

3. The studies of semileptonic decays that use large volumes of statistics make it possible to resolve the contradiction between exclusive and inclusive branching fractions of semileptonic decays of mesons and to measure the form-factors with a high accuracy.

4. Many new discoveries are to be expected in the spectroscopy of charmed particles, primarily in the spectroscopy of charmed baryons. Charmed particles with double charm constitute a new, interesting area of research.

5. The increase of the volume of statistics by a factor of several hundred will allow researchers to investigate many rare processes that exist within the SM or lie outside the scope of that model. This will also make it possible study the effect of CP-symmetry violation in the decays of D mesons, in $D^0\bar{D}^0$ mixing, etc.

The past decades have been extremely productive in new discoveries in the physics of charmed particles. There is every reason to believe that years to come will bring many new, interesting results.

Acknowledgements
I am deeply grateful to L B Okun' for carefully reading the manuscript and for valuable comments and to M V Danilov for useful discussions. I would also like to thank S Ya Barsuk for the help at the stage of preparation of the manuscript for press.

References

1. Bjorken J D, Glashow S L *Phys. Lett.* **11** 255 (1964); Gell-Mann M *Phys. Lett.* **8** 214 (1964); Tarjanne P, Teplitz V *Phys. Rev. Lett.* **11** 447 (1963); Hara Y *Phys. Rev.* **134** B214 (1964); Amati D et al. *Phys. Lett.* **11** 190 (1964)
2. Vladimirskii V V, Preprints ITEP-262, 299 (Moscow: Institute of Theoretical and Experimental Physics, 1964); Preprint ITEP-353 (Moscow: Institute of Theoretical and Experimental Physics, 1965)
3. Okun L B *Phys. Lett.* **12** 250 (1964)
4. Glashow S L, Iliopoulous J, Maiani L *Phys. Rev. D* **2** 1285 (1970)
5. Okun' L B *Leptony i Kvarki* (Leptons and Quarks, 2nd ed.) (Moscow: Nauka, 1981) [Translated into English (Amsterdam: North-Holland, 1984)]
6. Aubert J et al. *Phys. Rev. Lett.* **33** 1402 (1974)
7. Augustin J-E et al. *Phys. Rev. Lett.* **33** 1406 (1974)
8. Abrams G S et al. *Phys. Rev. Lett.* **33** 1953 (1974)
9. Braunschweig W et al. *Phys. Lett. B* **57** 407 (1975)
10. Goldhaber G et al. *Phys. Rev. Lett.* **37** 255 (1976)
11. Peruzzi I et al. *Phys. Rev. Lett.* **37** 569 (1976)
12. Maglich B (Ed.) *Adventures in Experimental Physics* Vol. 5 *Epsilon* (Princeton, N.J.: World Science Education, 1976)
13. Frixione S, Mangano M L, Nason P, Ridolfi G, hep-ph/9702287 (1997)
14. Toki W, in *Invited Talk at the Workshop on Charm Physics, Beijing, China, 1987* (CCAST (World Laboratory) Symposium/Workshop Proc., Vol. 2, Eds M Ye, T Huang) (New York: Gordon and Breach Science Publ., 1988) p. 89; Cords D *Lecture Presented at the Int. School of Elementary Particle Physics, Kupari-Dubrovnik, Yugoslavia* (1977)
15. Bernstein D et al. *Nucl. Instrum. Methods A* **226** 301 (1984)
16. Bai J Z et al. *Nucl. Instrum. Methods A* **344** 319 (1994); Bai J Z et al. *Phys. Rev. Lett.* **69** 3021 (1992)
17. Albrecht H et al. *Nucl. Instrum. Methods A* **275** 1 (1989)
18. Andrews D et al. *Nucl. Instrum. Methods A* **211** 47 (1989)
19. Kubota Y et al. *Nucl. Instrum. Methods A* **320** 66 (1992)
20. Decamp D et al. *Nucl. Instrum. Methods A* **294** 121 (1990)
21. Abreu P et al. *Nucl. Instrum. Methods A* **303** 233 (1991); **378** 57 (1996)
22. Adeva B et al. *Nucl. Instrum. Methods A* **289** 35 (1990); Adriani O A et al. *Nucl. Instrum. Methods A* **302** 53 (1991); Deiters K et al. *Nucl. Instrum. Methods A* **323** 162 (1992)
23. Ahmet K et al. *Nucl. Instrum. Methods A* **305** 275 (1991)
24. Albrecht H et al. *Phys. Rep.* **276** 223 (1996)
25. Raab J R et al. *Phys. Rev. D* **37** 2391 (1988)
26. Frabetti P L et al. *Nucl. Instrum. Methods A* **320** 519 (1992)
27. Alves G A et al. *Phys. Rev. Lett.* **69** 3147 (1992)
28. Amato S et al. *Nucl. Instrum. Methods A* **324** 535 (1993)

29. Alexandrov Yu A et al. *Nucl. Instrum. Methods A* **324** 535 (1998)
30. Gaillard M K, Lee B W, Rosner J L *Rev. Mod. Phys.* **47** 277 (1975); Ellis J, Gaillard M K, Napoulos D V *Nucl. Phys. B* **100** 313 (1975); Fakirov D, Stech B *Nucl. Phys. B* **133** 1315 (1978); Cabibbo N, Maiani L *Phys. Lett. B* **73** 418 (1978)
31. Chen A et al. *Phys. Rev. Lett.* **51** 634 (1983)
32. Althoff M et al. *Phys. Lett. B* **136** 130 (1984)
33. Albrecht H et al. *Phys. Lett. B* **153** 343 (1985)
34. "Review of Particle Physics" *Europ. Phys. J. C* **3** 1 (1996)
35. Goldhaber et al. *Phys. Lett. B* **69** 503 (1977)
36. Glashow Sh L "Towards a unified theory — threads of a tapestry," Nobel Lecture, December 8, 1979; Salam A "Gauge unification of fundamental forces," Nobel Lecture, December 8, 1979; Weinberg S "Conceptual foundation of the unified theory of weak and electromagnetic interactions," Nobel Lecture, December 8, 1979
37. Bartelt J et al. *Phys. Rev. Lett.* **80** 3919 (1998)
38. Himel T et al. *Phys. Rev. Lett.* **44** 920 (1980)
39. Albrecht H et al. *Phys. Lett. B* **146** 111 (1984)
40. Gronberg J et al. *Phys. Rev. Lett.* **75** 3232 (1995)
41. Isgur N, Wise M B *Phys. Rev. Lett.* **66** 1130 (1991)
42. Rosner J L *Comments Nucl. Part. Phys.* **16** 109 (1986)
43. Albrecht H et al. *Phys. Rev. Lett.* **56** 549 (1986)
44. Albrecht H et al. *Phys. Lett. B* **221** 422 (1989); **230** 162 (1989); **231** 208 (1989); **232** 398 (1989); **297** 425 (1992); *Z. Phys. C* **69** 405 (1996)
45. Avery P et al. *Phys. Rev. D* **41** 774 (1990); *Phys. Lett. B* **303** 377 (1993); **331** 236 (1994); **340** 194 (1994); Kubota Y et al. *Phys. Rev. Lett.* **72** 1972 (1994)
46. Anjos J C et al. *Phys. Rev. Lett.* **62** 1717 (1989)
47. Frabetti P L et al. *Phys. Rev. Lett.* **72** 324 (1994)
48. Akers R et al. *Z. Phys. C* **67** 57 (1995); Buskulic D et al. *Phys. Lett. B* **345** 103 (1994); *Z. Phys. C* **62** 1 (1994); *Z. Phys. C* **73** 601 (1997)
49. Besson D, in *Proc. of Int. Europhysics Conf. on HEP, Jerusalem* (1997)
50. Biagi S et al. *Z. Phys. C* **28** 175 (1985)
51. Albrecht H et al. *Phys. Lett. B* **288** 367 (1992); Stiewe J, in *Proc. of 26th Int. Conf. on HEP, New York* (1993) p. 1076
52. Frabetti P L et al. *Phys. Lett. B* **300** 190 (1993)
53. Frabetti P L et al. *Phys. Lett. B* **338** 106 (1994)
54. Siebert H W, in *Invited Talk at Production and Decay of Hyperons Charm and Beauty Hadrons, Strasbourg, France,* 1995; *Nucl. Phys. Proc. Suppl.* **50** 162 (1996)
55. Ammosov V V et al. *Pis'ma Zh. Eksp. Teor. Fiz.* **58** 241 (1993) [*JETP Lett.* **58** 247 (1993)]
56. Avery P et al. *Phys. Rev. Lett.* **75** 4364 (1995); Gibbons L et al. *Phys. Rev. Lett.* **77** 810 (1996); Brandenburg G et al. *Phys. Rev. Lett.* **78** 2304 (1997)
57. Albrecht H et al. *Phys. Lett. B* **317** 227 (1993)
58. Edwards K W et al. *Phys. Rev. Lett.* **74** 3331 (1995); Frabetti P L et al. *Phys. Rev. Lett.* **72** 961 (1994)
59. Frabetti P L et al. *Phys. Lett. B* **323** 459 (1994); *Phys. Rev. Lett.* **70** 1381, 1775, 2058 (1993); **71** 827 (1993)
60. Albrecht H et al. *Phys. Lett. B* **210** 267 (1988)
61. Prell S, in *Talk at XXXIII Recontres de Moriond, QCD and High Energy Hadronic Interactions, Les Arcs, France,* 1998
62. Frabetti P L et al. *Phys. Lett. B* **357** 678 (1995)
63. Adamovich M I et al. *Phys. Lett. B* **358** 151 (1995)
64. Bellini G, Bigi I I, Dornan P J *Phys. Rep.* **289** 1 (1998)
65. Guberina B, Ruckl R, Trampetic J *Z. Phys. C* **33** 297 (1986)
66. Voloshin M B, Shifman M A *Zh. Eksp. Teor. Fiz.* **91** 1180 (1986) [*Sov. Phys. JETP* **64** 698 (1986)]
67. Blok B, Shifman M, in *Proc. of the Third Workshop on the Phys. at a Tau-Charm Factory, Marbella, Spain, June 1993* (Ed. R J Kirkby) (Editions Frontieres, 1994)
68. Richman J D, Burchat P R *Rev. Mod. Phys.* **67** 893 (1995)
69. Kobayashi M, Maskawa T *Prog. Theor. Phys.* **49** 652 (1973)
70. Rosner J L *Phys. Rev. D* **42** 3732 (1990); Colangelo P, Nardulli G, Pietroni M *Phys. Rev. D* **43** 3002 (1991); Dominguez C A, in *Workshop on QCD: 20 Years Later, Aachen, Germany, June* 9 – 13 1991; Shigemitsu J, in *Proc. of 27th Int. Conf. on HEP, Glasgow* (1994) p. 135
71. Aoki S et al. *Prog. Theor. Phys.* **89** 131 (1993)
72. Acosta D et al. *Phys. Rev. D* **49** 5690 (1994)
73. Chadha M et al. *Phys. Rev. D* **58** 3202 (1998)
74. Kodama K et al. *Phys. Lett. B* **382** 299 (1996)
75. Bai J Z et al. *Phys. Rev. Lett.* **74** 4599 (1995)
76. Kodama K et al. *Phys. Lett. B* **309** 483 (1993)
77. Acciarri M et al. *Phys. Lett. B* **396** 327 (1997)
78. Adler J et al. *Phys. Rev. Lett.* **60** 1375 (1988)
79. Bai J Z et al., SLAC-PUB-7147 (1996)
80. Baltrusaitis R M et al. *Phys. Rev. Lett.* **54** 1976 (1985)
81. Kodama K et al. *Phys. Lett. B* **336** 605 (1994)
82. Albrecht H et al. *Phys. Lett. B* **374** 249 (1996)
83. Kubota Y et al. *Phys. Rev. D* **54** 2994 (1996)
84. Abachi S et al. *Phys. Lett. B* **205** 411 (1988)
85. Wirbel M et al. *Z. Phys. C* **29** 637 (1985); Korner J G, Schuler G A *Z. Phys. C* **38** 511 (1988); Isgur N et al. *Phys. Rev. D* **39** 799 (1989)
86. Ball P, Braun Y M, Dosch H G *Phys. Rev. D* **44** 3567 (1991)
87. Scora D, Isgur N *Phys. Rev. D* **52** 2783 (1995)
88. Lubicz V et al. *Phys. Rev. B* **274** 415 (1992)
89. Brandenburg G et al. *Phys. Rev. Lett.* **75** 3804 (1995); Abada A et al. *Nucl. Phys. B* **416** 675 (1994); Allton C R et al. *Phys. Lett. B* **345** 513 (1995)
90. Isgur N, Wise M B *Phys. Rev. D* **42** 2388 (1990)
91. Butler F et al. *Phys. Rev. D* **52** 2656 (1995)
92. Frabetti P L et al. *Phys. Lett. B* **382** 312 (1996)
93. Adler J et al. *Phys. Rev. Lett.* **62** 1821 (1989)
94. Bartelt J et al. *Phys. Lett. B* **405** 373 (1997)
95. Kodama K et al. *Phys. Lett. B* **316** 455 (1993)
96. Frabetti P L et al. *Phys. Lett. B* **391** 235 (1997)
97. Aitala E M et al. *Phys. Lett. B* **397** 325 (1997)
98. Bajc B, Fajfer S, Oakes R J *Phys. Rev. D* **53** 4957 (1996); Casalbuoni R et al. *Phys. Lett. B* **299** 139 (1993); Ball P *Phys. Rev. D* **48** 3190 (1993)
99. Albrecht H et al. *Phys. Lett. B* **269** 234 (1991); *Phys. Lett. B* **303** 368 (1993)
100. Bergfeld T et al. *Phys. Lett. B* **323** 219 (1994); Alexander J P et al. *Phys. Rev. Lett.* **74** 3113 (1995)
101. Vella E et al. *Phys. Rev. Lett.* **48** 1515 (1982)
102. Ballagh H C et al. *Phys. Rev. D* **24** 7 (1981)
103. Anjos J C et al. *Phys. Rev. Lett.* **62** 722 (1989)
104. Frabetti P L et al. *Phys. Lett. B* **307** 262 (1993)
105. Anjos J C et al. *Phys. Rev. Lett. D* **45** R2177 (1992)
106. Kodama K et al. *Phys. Lett. B* **313** 260 (1993)
107. Adler J et al. *Phys. Rev. Lett.* **60** 89 (1988)
108. Albrecht H et al. *Phys. Lett. B* **340** 125 (1994); Akerib D S et al. *Phys. Rev. Lett.* **71** 3070 (1994); Barate R et al. *Phys. Lett. B* **403** 367 (1997)
109. Gibbons L et al. *Phys. Rev. Lett.* **77** 810 (1996)
110. Bai J Z et al. *Phys. Rev. D* **52** 3781 (1995)
111. Artuso M et al. *Phys. Lett. B* **378** 364 (1996)
112. Bigi I I, Fukugita M *Phys. Lett. B* **91** 121 (1980)
113. Albrecht H et al. *Phys. Lett. B* **158** 525 (1985)
114. Albrecht H et al. *Z. Phys. C* **33** 359 (1987)
115. Lipkin H J *Phys. Lett. B* **90** 710 (1980); Bauer M, Stech B *Phys. Lett. B* **152** 380 (1985); Donoghue J F *Phys. Rev. D* **33** 1516 (1986)
116. Bauer M, Stech B, Wirbel M *Z. Phys. C* **34** 103 (1987)
117. Wirbel M *Nucl. Phys. B* **268** 33 (1988)
118. Abrams G S et al. *Phys. Rev. Lett.* **43** 481 (1979)
119. Baltrusaitis R M et al. *Phys. Rev. Lett.* **55** 150 (1985)
120. Blok B Yu, Shifman M A *Yad. Fiz.* **45** 211, 478, 841 (1987) [*Sov. J. Nucl. Phys.* **45** 135, 301, 522 (1987)]
121. Wolfenstein L *Phys. Lett. B* **164** 170 (1985); Kaeding T A *Phys. Lett. B* **357** 151 (1995)
122. Gaillard M K, Lee B W *Phys. Rev. D* **10** 897 (1974); Datta A *Phys. Lett. B* **154** 287 (1985)
123. Donoghue J et al. *Phys. Rev. D* **33** 179 (1986)
124. Gladding G E, in *Proc. of the Fifth Int. Conf. on Phys. in Collision, Autun, France, 1985*
125. Bigi I, Sanda A I *Phys. Lett. B* **171** 320 (1986); Chau L L, Cheng H Y *Phys. Lett. B* **280** 281 (1992)
126. Anjos J C et al. *Phys. Rev. Lett.* **60** 1239 (1988)
127. Blaylock G, Seiden A, Nir Y *Phys. Lett. B* **355** 555 (1995); Wolfenstein L *Phys. Rev. Lett.* **75** 2460 (1995)
128. Aitala E M et al. *Phys. Rev. D* **57** 13 (1998)
129. Cinabro D et al. *Phys. Rev. Lett.* **72** 1406 (1994)
130. Frabetti P L et al. *Phys. Lett. B* **354** 486 (1995)
131. Aitala E M et al. *Phys. Lett. B* **404** 187 (1997)

132. Liu T, in *Proc. of the Workshop on the Tau/Charm Factory, Argonne,* 1995; hep-ph/9508415.
133. Louis W C et al. *Phys. Rev. Lett.* **56** 1027 (1986)
134. Carter A B, Sanda A I *Phys. Rev. Lett.* **45** 952 (1980); *Phys. Rev. D* **23** 1567 (1981); Bigi I I, Sanda A I *Nucl. Phys. B* **193** 85 (1981); **281** 41 (1987)
135. Semenov S, in *Proc. of Int. Europhysics Conf. on HEP, Jerusalem* (*1997*)
136. Golden M, Grinstein B *Phys. Lett. B* **222** 501 (1989); Close F E, Lipkin N J *Phys. Lett. B* **372** 306 (1996)
137. Le Yaouanc A, Oliver L, Raynal J-C *Phys. Lett. B* **292** 353 (1992)
138. Anjos J C et al. *Phys. Rev. D* **44** R3371 (1991)
139. Frabetti P L et al. *Phys. Rev. D* **44** R2953 (1994)
140. Bartelt J et al. *Phys. Rev. D* **52** 4860 (1995)
141. Aitala E M et al. *Phys. Lett. B* **403** 377 (1997); **421** 405 (1998)
142. Hewett J L, hep-ph/9505246 (1995)
143. Freyberger A et al. *Phys. Rev. Lett.* **76** 3065 (1996)
144. Adamovich M et al. *Phys. Lett. B* **353** 563 (1995)
145. Kodama K et al. *Phys. Lett. B* **345** 85 (1995)
146. Aitala E M et al. *Phys. Rev. Lett.* **76** 364 (1996)
147. Frabetti P L et al. *Phys. Lett. B* **398** 239 (1997)
148. Haas P et al. *Phys. Rev. Lett.* **60** 1614 (1988)
149. Preprint CLNS 94/1277, 1994
150. Procario M, in *Proc. of Int. of Particle and Nuclear Phys., Montana, 1997*
151. Cheung H W K *Invited Talk at Production and Decay of Hyperons Charm and Beauty Hadrons, Strasbourg, France, 1995*; *Nucl. Phys. Proc. Suppl.* **50** 154 (1996)
152. Baum G et al., Preprint CERN-SPSLC-96-14 (1996)
153. Kaplan D M *Invited Talk at Production and Decay of Hyperons Charm and Beauty Hadrons, Strasbourg, France, 1995*; *Nucl. Phys. Proc. Suppl.* **50** 260 1996
154. Kirkby J, Preprint CERN-PPE-96-112 (1996)